Article

Cell Host & Microbe

# *Pseudomonas syringae* Type III Effector HopBB1 Promotes Host Transcriptional Repressor Degradation to Regulate Phytohormone Responses and Virulence

## Graphical Abstract

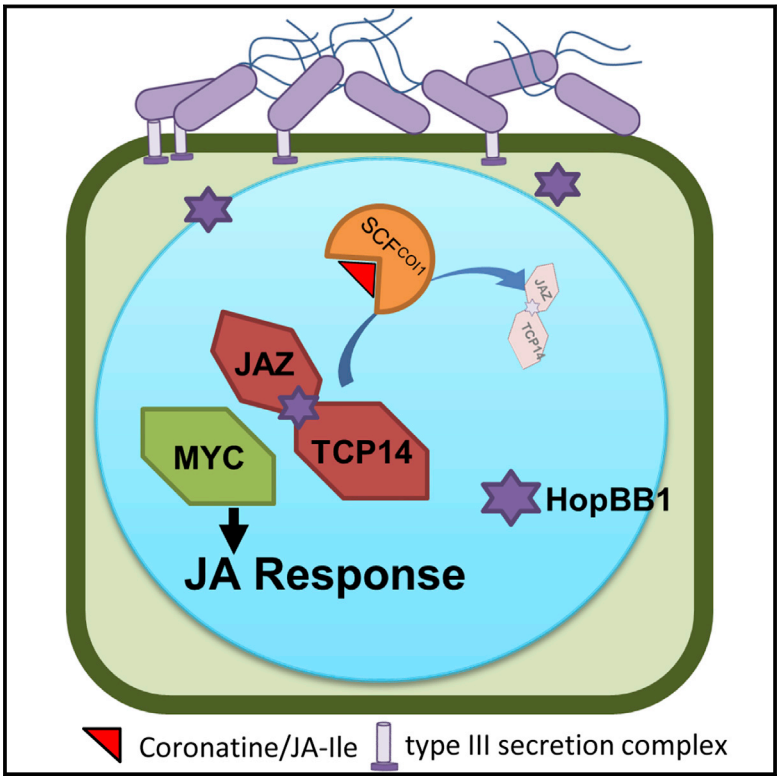


## Authors

Li Yang,
Paulo José Pereira Lima Teixeira,
Surojit Biswas, ..., Petra Epple,
Piotr Mieczkowski, Jeffery L. Dangl

## Correspondence

dangl@email.unc.edu

## In Brief

Yang et al. demonstrate that the *Pseudomonas syringae* type III effector HopBB1 modulates two negative regulators of plant jasmonic acid (JA) signaling, TCP14 and JAZ3, and "glues" them together for degradation, resulting in precise activation of a subset of JA output responses that promote bacterial virulence.

## Highlights

- The transcriptional regulator TCP14 represses JA response to promote disease resistance
- The *Pseudomonas syringae* type III effector HopBB1 interacts with TCP14
- HopBB1 activates TCP14-repressed JA response genes and promotes bacterial virulence
- HopBB1 targets TCP14 for $SCF^{COI1}$-dependent degradation by connecting it to JAZ3

## Accession Numbers

GSE90606

Yang et al., 2017, Cell Host & Microbe *21*, 1–13
February 8, 2017 
http://dx.doi.org/10.1016/j.chom.2017.01.003

CellPress

Please cite this article in press as: Yang et al., *Pseudomonas syringae* Type III Effector HopBB1 Promotes Host Transcriptional Repressor Degradation to Regulate Phytohormone Responses and Virulence, Cell Host & Microbe (2017), http://dx.doi.org/10.1016/j.chom.2017.01.003

Cell Host & Microbe
Article

# *Pseudomonas syringae* Type III Effector HopBB1 Promotes Host Transcriptional Repressor Degradation to Regulate Phytohormone Responses and Virulence

Li Yang,[1,2,6] Paulo José Pereira Lima Teixeira,[1,2,6] Surojit Biswas,[1,2,7] Omri M. Finkel,[1,2] Yijian He,[1,2,8] Isai Salas-Gonzalez,[1,2] Marie E. English,[1,9] Petra Epple,[1,2,10] Piotr Mieczkowski,[3] and Jeffery L. Dangl[1,2,3,4,5,11,*]
[1]Howard Hughes Medical Institute
[2]Department of Biology
[3]Carolina Center for Genome Science
[4]Department of Microbiology and Immunology
[5]Curriculum in Genetics and Molecular Biology
University of North Carolina at Chapel Hill, Chapel Hill, NC 27599, USA
[6]Co-first author
[7]Present address: Department of Biomedical Informatics, Harvard Medical School, Boston, MA 02215, USA
[8]Present address: Department of Plant Pathology, NC State University, Raleigh, NC 27695, USA
[9]Present address: Department of Biosystems Engineering and Soil Science, University of Tennessee, Knoxville, TN 37996, USA
[10]Present address: BASF Plant Science LP, Research Triangle Park, NC 27709, USA
[11]Lead Contact
*Correspondence: dangl@email.unc.edu
http://dx.doi.org/10.1016/j.chom.2017.01.003

## SUMMARY

**Independently evolved pathogen effectors from three branches of life (ascomycete, eubacteria, and oomycete) converge onto the *Arabidopsis* TCP14 transcription factor to manipulate host defense. However, the mechanistic basis for defense control via TCP14 regulation is unknown. We demonstrate that TCP14 regulates the plant immune system by transcriptionally repressing a subset of the jasmonic acid (JA) hormone signaling outputs. A previously unstudied *Pseudomonas syringae* (*Psy*) type III effector, HopBB1, interacts with TCP14 and targets it to the $SCF^{COI1}$ degradation complex by connecting it to the JA signaling repressor JAZ3. Consequently, HopBB1 de-represses the TCP14-regulated subset of JA response genes and promotes pathogen virulence. Thus, HopBB1 fine-tunes host phytohormone crosstalk by precisely manipulating part of the JA regulon to avoid pleiotropic host responses while promoting pathogen proliferation.**

## INTRODUCTION

A robust immune system defends plants against most microbes. Plants deploy surface-localized pattern recognition receptors to detect conserved microbe-associated molecular patterns (MAMPs), which leads to the activation of MAMP-triggered immunity (MTI). To counteract MTI, pathogenic microbes deploy virulence factors, often termed effector proteins, into plant cells, where they interact with host factors to subvert defense responses or to alter nutrition distribution. To counteract effector protein action, plants evolved a large, polymorphic family of intra-cellular receptors with a nucleotide-binding domain and leucine-rich repeats, termed NLRs. Plant NLR receptors are analogous to animal NLR innate immune receptors. NLR receptors in both kingdoms are activated either by direct interactions with ligands, including effector proteins, or by recognition of effector-modified host cellular machines that are the nominal effector targets or decoys of those targets (Bentham et al., 2016;Jones and Dangl, 2006; van der Hoorn and Kamoun, 2008). NLR activation initiates effector-triggered immunity (ETI). Deciphering the mechanisms by which effector repertoires from divergent pathogens act will provide a more comprehensive view of the host cellular machinery responsible for plant immune system function.

Interactome studies revealed that candidate effector repertoires from three evolutionarily diverse pathogens—*P. syringae* (*Psy;* eubacteria), *H. arabidopsidis* (*Hpa*; oomycete), and *Golovinomyces orontii* (*Go*; ascomycete)—converge onto a limited set of interconnected *Arabidopsis* proteins (Dreze et al., 2011; Mukhtar et al., 2011; Weßling et al., 2014). TCP14, a transcription factor belonging to the conserved TCP (teosinte branched1, CYCLOIDEA, PROLIFERATING CELL FACTORS 1 and 2) family, is one of the convergent host targets. The reference *Arabidopsis* Col-0 genome encodes 24 TCP family members that share a basic helix-loop-helix (bHLH) domain (the TCP domain) and are versatile regulators of plant development and hormone signaling (Lopez et al., 2015). TCP14 physically interacts with SRFR1 and contributes to effector-triggered immunity (Kim et al., 2014). In various tissues, TCP14 promotes cytokinin and gibberellic acid growth hormone responses (Kieffer et al., 2011; Resentini et al., 2015; Steiner et al., 2012). TCP14 is localized to sub-nuclear foci and its co-expression resulted in the re-localization of 22/33 tested nuclear-localized effectors from the three pathogens noted above (Weßling et al., 2014). Additionally, the phytoplasma SAP11 effector associates with

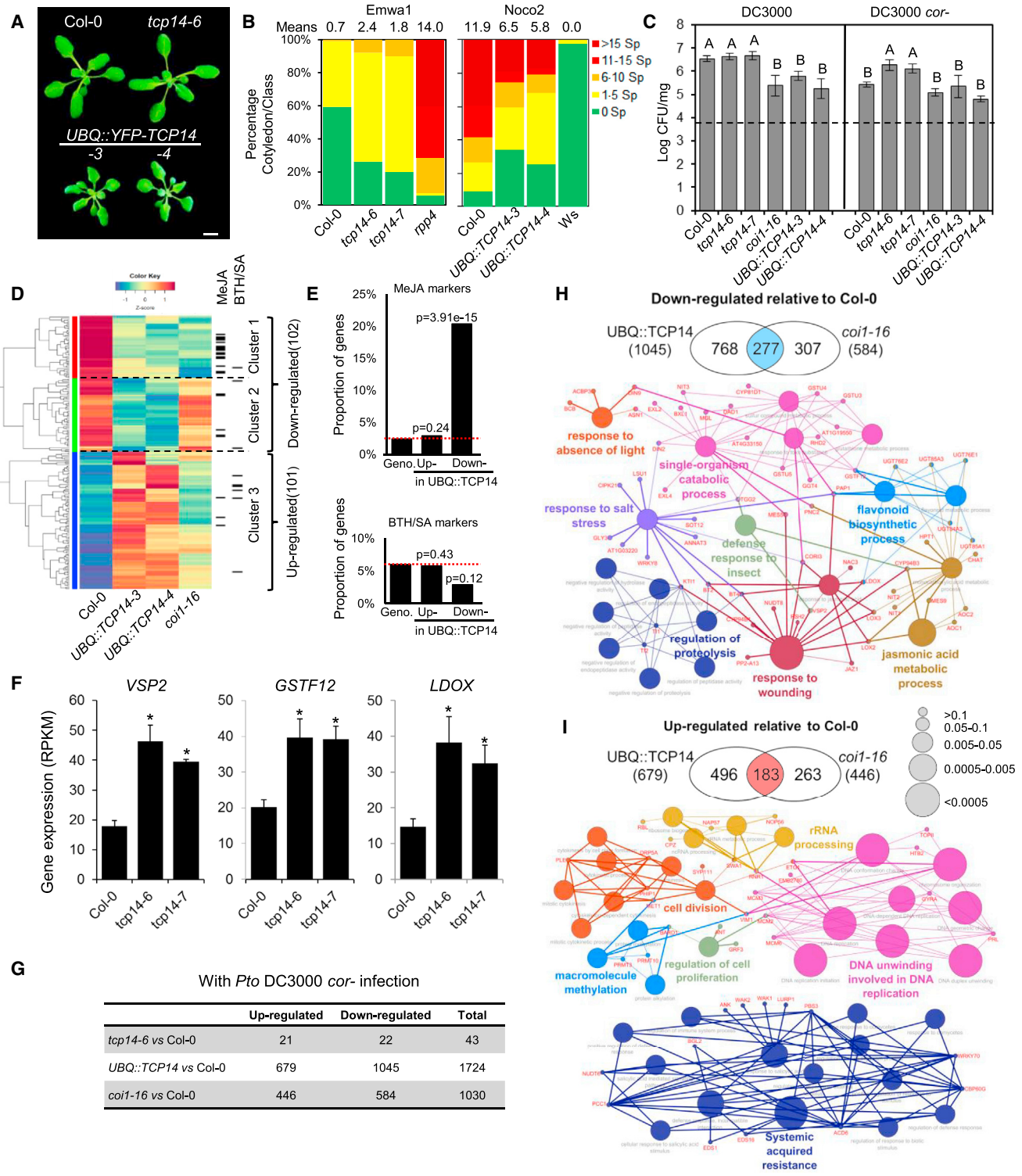


| | Up-regulated | Down-regulated | Total |
|---|---|---|---|
| *tcp14-6 vs* Col-0 | 21 | 22 | 43 |
| *UBQ::TCP14 vs* Col-0 | 679 | 1045 | 1724 |
| *coi1-16 vs* Col-0 | 446 | 584 | 1030 |

**Figure 1. TCP14 Represses JA Response and Promotes Disease Resistance**

(A) Shown are 3-week-old plants of Col-0, *tcp14-6*, *UBQ::YFP-TCP14-3* and *UBQ::YFP-TCP14-4*. Scale bar represents 5 mm.

(B) *tcp14* mutants are more susceptible to *Hpa* Emwa1 than Col-0. Overexpressing TCP14 in *Arabidopsis* enhances disease resistance against *Hpa* Noco2. The means represent the numbers of sporangiophores (sp) on each cotyledon (n > 50).

(C) Mutation in *TCP14* enhances the virulence of DC3000 *cor*−. The 2-week-old plants were dip inoculated with indicated bacteria strains at $OD_{600}$ = 0.05. CFU indicates bacterial colony formation units; error bars represent ± SD.

*(legend continued on next page)*

other members of the TCP family to repress JA biosynthesis, which ultimately enhances the feeding behavior of its insect vector, the leaf hopper (Sugio et al., 2011).

Plant cells integrate growth and division cues with defense cues via phytohormone signaling interactions (Belkhadir et al., 2014; Robert-Seilaniantz et al., 2011). The antagonistic regulatory relationship between the defense hormones jasmonic acid (JA) and salicylic acid (SA) endows a plant with the flexibility to prioritize defense responses against pathogens with diverse lifestyles (Robert-Seilaniantz et al., 2011). In *Arabidopsis*, activation of SA-dependent responses limits the growth of biotrophic or hemibiotrophic pathogens. On the other hand, JA-dependent responses limit the growth of necrotrophic pathogens and herbivorous insects. Hence, biotrophic or hemibiotrophic pathogens inhibited by SA-mediated immune responses will benefit from activation of JA-dependent responses (Browse, 2009; He et al., 2004; Zheng et al., 2012). Host cellular machines regulating the SA-JA balance are therefore attractive targets for effectors that mimic the action of either hormone, misdirect the defense response, and thus facilitate pathogen or pest proliferation (Kazan and Lyons, 2014).

The transcriptional outputs of JA response are repressed by a group of JASMONATE ZIM DOMAIN (JAZ) proteins through their association with transcription factors (Chini et al., 2007; Zhang et al., 2015). Three MYC transcription factors (MYC2, MYC3, and MYC4) repressed by JAZ proteins are positive regulators of JA-mediated responses in *Arabidopsis* (Kazan and Manners, 2013). JAZ proteins directly or indirectly recruit a transcription co-repressor complex containing Topless (TPL) and histone deacetylase to repress MYC activity (Pauwels et al., 2010). JA biosynthesis is induced during normal development or following either MAMP treatment or *Pseudomonas syringae* infection (Lewis et al., 2015; Schmelz et al., 2003). JAZ proteins bind isoleucine-conjugated JA, which facilitates their physical interaction with the CORONATINE-INSENSITIVE 1 (COI1) F-box component of a Skip-cullin-F-box (SCF)-type E3 ubiquitin ligase (Sheard et al., 2010). This results in proteasome-mediated degradation of JAZ proteins and allows MYC-dependent activation of JA response genes (Thines et al., 2007; Wasternack and Hause, 2013). The MYC regulon controls a pleiotropic physiological and developmental response including the repression of SA-dependent transcriptional output (Kazan and Manners, 2013).

At least two *Psy* type III effectors, HopX1 and HopZ1a, and the phytotoxin coronatine can activate the JA pathway. Coronatine is a structural mimic of JA-Ile (Katsir et al., 2008). HopX1 is a cysteine protease that eliminates JAZ proteins by cleaving their central ZIM domain (Gimenez-Ibanez et al., 2014). HopZ1a is an acetyltransferase that acetylates soybean and *Arabidopsis* JAZ proteins, promoting COI1-dependent JAZ turnover (Jiang et al., 2013). Both HopX1 and HopZ1a were identified from *Psy* strains deficient in coronatine biosynthesis, and each can rescue the growth defects of a *Psy* mutant unable to synthesize coronatine (Gimenez-Ibanez et al., 2014; Jiang et al., 2013). Effects of HopX1 or HopZ1a action on the global, JA-activated transcriptional landscape have not been defined, though each causes de-repression of a few tested JA response genes (Gimenez-Ibanez et al., 2014; Jiang et al., 2013).

Here, we provide a mechanistic model for how one of the many TCP14-targeting effectors suppresses defense by manipulating the host defense hormone network to promote *Psy* virulence. Our data demonstrate that the previously unstudied bacterial type III effector, HopBB1, alters subsets of targets from two heretofore unlinked transcriptional regulons, TCP14 and MYC, to de-repress a subset of JA responses and promote virulence while avoiding pleiotropic effects associated with full misregulation of either regulon.

## RESULTS

### TCP14 Is a Negative Regulator of JA Signaling

We showed that a *tcp14* mutant enhanced susceptibility to the avirulent Emwa1 isolate of the oomycete pathogen, *Hpa* (Mukhtar et al., 2011; Weßling et al., 2014). We confirmed and extended this result using a second *tcp14* allele and transgenic *Arabidopsis* overexpressing YFP-TCP14 from the *UBQ* promoter (Figures 1A and 1B). These plants were modestly smaller than wild-type plants at the same developmental stage (Figures 1A and S1A) and displayed enhanced disease resistance when challenged with the virulent *Hpa* isolate Noco2 (Figure 1B). We examined the in planta growth of *P. syringae* pv. *tomato* strain DC3000 (*Pto* DC3000, hereafter DC3000) and a coronatine-deficient mutant, *Pto* DC3000 *cor*− (hereafter DC3000 *cor*−), on *tcp14* mutants and TCP14 overexpression lines. Plants overexpressing TCP14 displayed enhanced resistance to DC3000 at the same levels as *coi1* mutants (Figure 1C). The growth of DC3000 *cor*− was the same on Col-0 and plants overexpressing TCP14 (Figure 1C). *tcp14* mutants were unaltered in their response to DC3000 but rescued the growth defects of DC3000

(D) JA-responsive genes are repressed in 2-week-old TCP14-overexpressing plants. Shown is hierarchical clustering of the 203 genes identified as differentially expressed in the pairwise comparison between Col-0 and *UBQ::YFP-TCP14-3*. *UBQ::YFP-TCP14-4* and the *coi1-16* mutant were also included. MeJA- or BTH/SA-responsive genes (Table S1) are indicated on the right. Cluster 1 shows genes repressed in *UBQ::YFP-TCP14* and *coi1-16*; Cluster 2 shows genes repressed in *UBQ::YFP-TCP14*, but not in *coi1-16*; Cluster 3 shows genes upregulated in *UBQ::YFP-TCP14*.

(E) Genes downregulated in *UBQ::YFP-TCP14-3* are enriched for JA markers. Dashed lines represent the proportion of genes that belong to each group in the *Arabidopsis* genome. Geno (Genome) indicates the expected proportion of MeJA (or BTH/SA) markers in *Arabidopsis* genome; Up- or Down- indicates the proportion of MeJA (or BTH/SA) markers in genes upregulated or downregulated by *UBQ::YFP-TCP14*.

(F) Elevated expression of JA-responsive genes in steady-state *tcp14* mutants. * indicates FDR < 0.0001; error bars represent ± SD.

(G) Summary of transcriptional alterations in *tcp14-6*, *UBQ::YFP-TCP14* overexpression line and in *coi1-16* plants 24 hr after DC3000 *cor*− infection. The table depicts the number of differentially expressed genes in each line relative to infected wild-type plants.

(H) Gene ontology terms (biological processes) enriched in the set of 277 genes downregulated in both UBQ::YFP-TCP14 and *coi1-16* when compared to wild-type plants after infection. Note the prevalence of terms associated with the JA pathway. Gene names are labeled in red.

(I) Gene ontology terms (biological processes) enriched in the set of 183 genes upregulated in both UBQ::YFP-TCP14 and *coi1-16* when compared to wild-type plants after infection. Note the prevalence of terms associated with the SA pathway. Gene names are labeled in red. The complete GO enrichment results for (H) and (I) are shown in Table S2. See also Figure S1 and Tables S1 and S2.

*cor*− (Figure 1C). These disease phenotypes suggest that TCP14 regulates immune system output by suppressing the JA response.

To test the hypothesis that TCP14 is a negative regulator of the JA pathway, we defined a comprehensive set of marker genes for the JA and SA responses (Figures S1B–S1F; Table S1) and analyzed the transcriptomes of Col-0, *tcp14* mutants, and transgenic plants overexpressing TCP14 in 2-week-old seedlings; the time point when altered infection phenotypes were observed. A total of 203 genes were differentially expressed in TCP14-overexpressing seedlings compared to Col-0 (Figure 1D; Table S2). Genes downregulated by TCP14 overexpression were significantly enriched for genes that are activated by JA treatment (26/102; p = 2.19e-19, hypergeometric test; cluster 1, Figures 1D and 1E). Indeed, many of these downregulated genes were also weakly expressed in the *coi1-16* mutant (Figure 1D; Table S2). In contrast, only 6 of the 101 genes that were upregulated in the *UBQ::YFP-TCP14-3* line are markers of the SA response (Figure 1D), suggesting that TCP14-driven repression of the JA pathway was not a consequence of activated SA response. No global transcriptome changes were observed in *tcp14* mutants relative to Col-0 in non-infected plants (Table S2). However, some JA-responsive genes, including *VSP2* and those required for anthocyanin biosynthesis, were upregulated in the mutants (Figure 1F).

We also examined transcriptional alterations in these plants 24 hr after infection with DC3000 *cor*−. When compared to infected Col-0, both *coi1-16* and the *UBQ::YFP-TCP14-4* line showed weaker activation of JA-responsive genes (Figures 1G and 1H; Table S2). Although the suppression of the JA response is an obvious transcriptional alteration in either wild-type or infected *UBQ::YFP-TCP14* plants (Figures 1D and 1H), TCP14 may also participate in the regulation of other sectors of the plant immune system. Indeed, the enhanced disease phenotype in *UBQ::YFP-TCP14* also correlates with suppression of ABA-responsive genes and responses related to ABA signaling (Figure 1I, Table S2). Moreover, TCP14-overexpressing lines displayed enhanced activation of SA-responsive genes after infection (Figure 1I; Table S2), consistent with their enhanced resistance to both DC3000 and *Hpa* isolate Noco2 (Figures 1B and 1C). However, only 43 genes were differentially expressed in the infected *tcp14-6* mutant relative to wild-type plants (Figure 1G; Table S2). We do not know if the effects of *tcp14* mutation would be more dramatic at different time points in the response. Overall, this transcriptional profile supports the conclusion that TCP14 contributes to plant immunity as a negative regulator of subsets of the JA response.

## The *P. syringae* Effector HopBB1 Interacts with TCP14 In Vivo

To demonstrate how effectors modulate TCP14 function, we focused first on an uncharacterized TCP14-interacting *Psy* type III effector, HopBB1 (Mukhtar et al., 2011). In yeast, HopBB1 selectively interacts with a subset of 24 *Arabidopsis* TCP family members (Figure S2A). We validated the interactions between HopBB1 and TCP14 in planta by inoculating YFP-TCP14 overexpressing *Arabidopsis* with DC3000 *cor*− expressing HopBB1-HA at native levels. We observed that HopBB1-HA was co-immunoprecipitated with YFP-TCP14 (Figure 2A), demonstrating that these two proteins associate in vivo during *Psy* infection. We used random mutagenesis to isolate a HopBB1 mutant, $HopBB1_{G126D}$ that lost interaction with TCP14 in yeast-two-hybridization (Y2H) and failed to associate with TCP14 in planta (Figures 2A, 2B, and S2B). $HopBB1_{111\text{-}283}$ that contains G126, but has no annotated function, was sufficient for association with TCP14 (Figure 2C). $TCP14_{180\text{-}489}$ downstream of the conserved TCP DNA binding domain was sufficient for interaction with HopBB1 in yeast and in planta (Figures 2D, 2E, and S2C). $TCP14_{180\text{-}216}$ co-immunoprecipitated with HopBB1 (Figure 2E). We replaced every six amino acids in this region with a structurally flexible sequence (NAAIRS; Wilson et al., 1985), and revealed that the TCP14 sequence motif 204-RSAAST-209 is necessary for interaction between full length TCP14 and HopBB1 (Figures 2F, 2G, and S2D). Collectively, these data are consistent with the hypothesis that HopBB1 associates with TCP14 in vivo.

## HopBB1 De-represses JA Response

We tested the hypothesis that HopBB1 targets TCP14 to manipulate plant JA response. Following delivery of native levels via type III secretion, HopBB1, but not $HopBB1_{G126D}$, partially rescued the growth defects of DC3000 *cor*− on Col-0 plants (Figures 3A and S3A). Growth promotion of DC3000 *cor*− contributed by HopBB1 was suppressed by overexpression of TCP14 and in *coi1* (Figure 3A). These observations indicate that HopBB1 partially complements the defects of coronatine deficiency, that this can be modulated by TCP14, and that it requires COI1.

We then investigated the effect of HopBB1 on the transcriptome of wild-type plants 24 hr after the infection. As expected, the transcriptome of plants infected with DC3000 was significantly different from those sprayed with either a mock or DC3000 *cor*− (EV) (Figures 3B and 3C). The set of 697 genes that were more strongly induced by DC3000 than by DC3000 *cor*− (EV) was enriched in biological processes related to JA and ABA responses (Table S3). Remarkably, infection with DC3000 *cor*− (HopBB1) resulted in a global transcriptional signature that resembled infection with DC3000 (Figure 3C), supporting our conclusion that HopBB1 can rescue the impaired ability of DC3000 *cor*− to establish infection. A total of 129 of the 672 (19%) JA-responsive genes were expressed to higher levels in plants infected with DC3000 or DC3000 *cor*− (HopBB1) than in plants with DC3000 *cor*− (EV) treatment. Although the transcriptional changes induced by DC3000 *cor*− ($HopBB1_{G126D}$) qualitatively resembled those induced by DC3000 (Figure 3C), these JA-responsive genes were less activated (p value = 2.2e−16, Student's t test), indicating that interaction with TCP14 is required for the full virulence function of HopBB1 (Figure 3D).

To exclude the possibility that the transcriptome change induced by bacteria-delivered HopBB1 may be confounded by other effectors that may influence JA signaling, we defined the transcriptome of transgenic plants expressing only HopBB1. As expected if HopBB1 potentiates JA responses, these plants were hypersensitive to JA-mediated inhibition of root elongation (Figure S3C). In addition, DC3000 *cor*− is more virulent on HopBB1 transgenic plants than on wild-type Col-0, demonstrating that heterologous HopBB1 complements this strain's coronatine deficiency (Figure 3F), analogous to *tcp14* (Figure 1C). We compared the transcriptome of HopBB1-expressing plants to Col-0 at steady state and identified 628 differentially

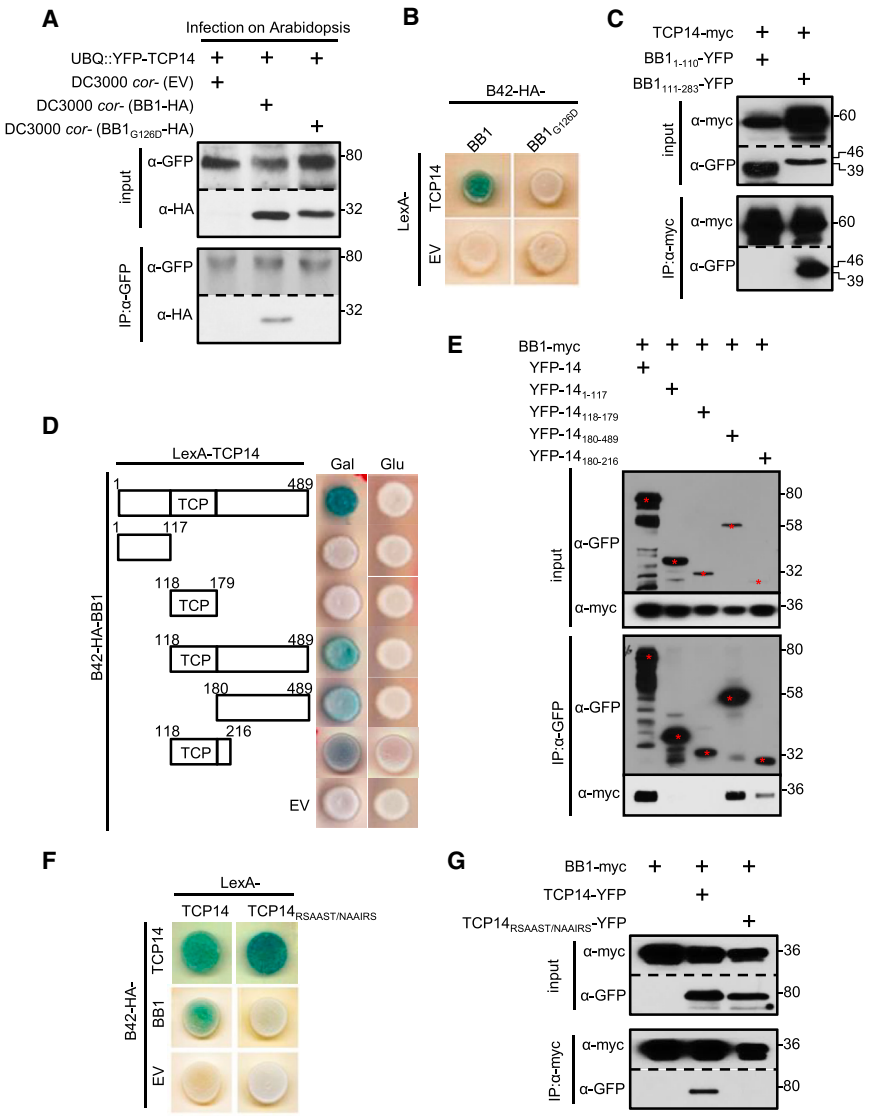


**Figure 2. HopBB1 Interacts with TCP14 In Planta**

(A) *Pto*-delivered HopBB1, but not HopBB1$_{G126D}$, associates with TCP14 in *Arabidopsis*. DC3000 *cor*− with empty vector (EV), HA-tagged HopBB1, or HopBB1$_{G126D}$ was hand-infiltrated at $OD_{600}$ = 0.05 into leaves of 4-week-old transgenic *Arabidopsis* expressing YFP-TCP14. Leaves were harvested 24 hr after inoculation.

(B) HopBB1$_{G126D}$ loses interaction with TCP14 in yeast.

(C) The C terminus (111–283) of HopBB1 is sufficient to associate with TCP14 in *N. benthamiana*.

(D) HopBB1 interacts with TCP14(aa180-216) in yeast.

(E) HopBB1 associates with TCP14$_{180-216}$ in *N. benthamiana*.

(F) TCP14$_{RSAAST/NAAIRS}$ fails to interact with HopBB1 in yeast but retains homodimerization.

(G) TCP14$_{RSAAST/NAAIRS}$ fails to associate with HopBB1 in *N. benthamiana*.

Proteins were transiently expressed in *N. benthamiana* from a 35S promoter for (C), (E), and (G). See also Figure S2.

expressed genes (593 upregulated and 35 downregulated) (Table S3). Many of our JA response marker genes (93/672; p = 3.41e−47; hypergeometric test) were upregulated in the HopBB1 expressing plants (Table S3), and the average expression of all 672 JA-responsive genes was higher in these transgenic plants (Figure 3G). JA response genes were enriched in the overlap between HopBB1-upregulated and TCP14-suppressed genes: out of the 102 genes that were downregulated by steady-state TCP14 overexpression (Figure 1D; Table S4), 12 were upregulated in HopBB1 transgenic plants and 10 of these are JA markers (p = 2.26e−17; hypergeometric test) (Table S4). Genes specific to BTH/SA response were also enriched in the HopBB1 upregulated genes (139/2,096; p = 2.53e−33; hypergeometric test). However, genes that are typically associated with SA-mediated defense responses (e.g., *PR-1*, *PR-5*, *ICS1*, and *WRKYs*) were not differentially expressed, suggesting that the SA response activated in HopBB1-expressing plants is likely to be insufficient for robust defense.

As expected, the JA response genes defined in our study were enriched for MYC2 binding motifs in their promoters (Figure S3D). In fact, these genes were enriched for co-occurrence of MYC2 and TCP binding sites (Franco-Zorrilla et al., 2014; Kosugi and Ohashi, 2002). Out of the 88 JA response genes that contain consensus MYC and TCP motifs in their promoters, 22 (25%) were also upregulated by HopBB1 expression (Figure S3E). Interestingly, neither constitutive nor conditional overexpression of HopBB1 caused the chlorotic leaf phenotype observed previously after either coronatine treatment or HopX1 expression (Figure S3F; Gimenez-Ibanez et al., 2014; Kloek et al., 2001). Consistent with this observation, the expression of MYC-dependent and JA-responsive photosynthetic genes (Qi et al., 2015) was not altered in HopBB1-expressing plants (Figure S3G). In sum, our transcriptome data are consistent with our pathology data and support the hypothesis that HopBB1 activates a sector of the overall JA response that is co-regulated by TCPs and MYC.

We surveyed the genomic distribution of *HopBB1*, coronatine biosynthetic genes, *HopX1*, and *HopZ1a* in 287 *Psy* genomes. Only four (1.3%) genomes contain two presumably functional JA-activating virulence factors (Figure 3H; Table S5). Nearly 50% (141) of *Psy* genomes carry one, and only one, functional version of these four JA-activating virulence factors (Figure 3H; Table S5). Strikingly, in a few additional cases where *HopX1* and coronatine biosynthetic genes co-exist in a single strain, the HopX1 alleles have mutations in functionally essential residues (Nimchuk et al., 2007). The phylogeny of the 141 *Psy* isolates suggests that independent gene gain and/or loss occurred

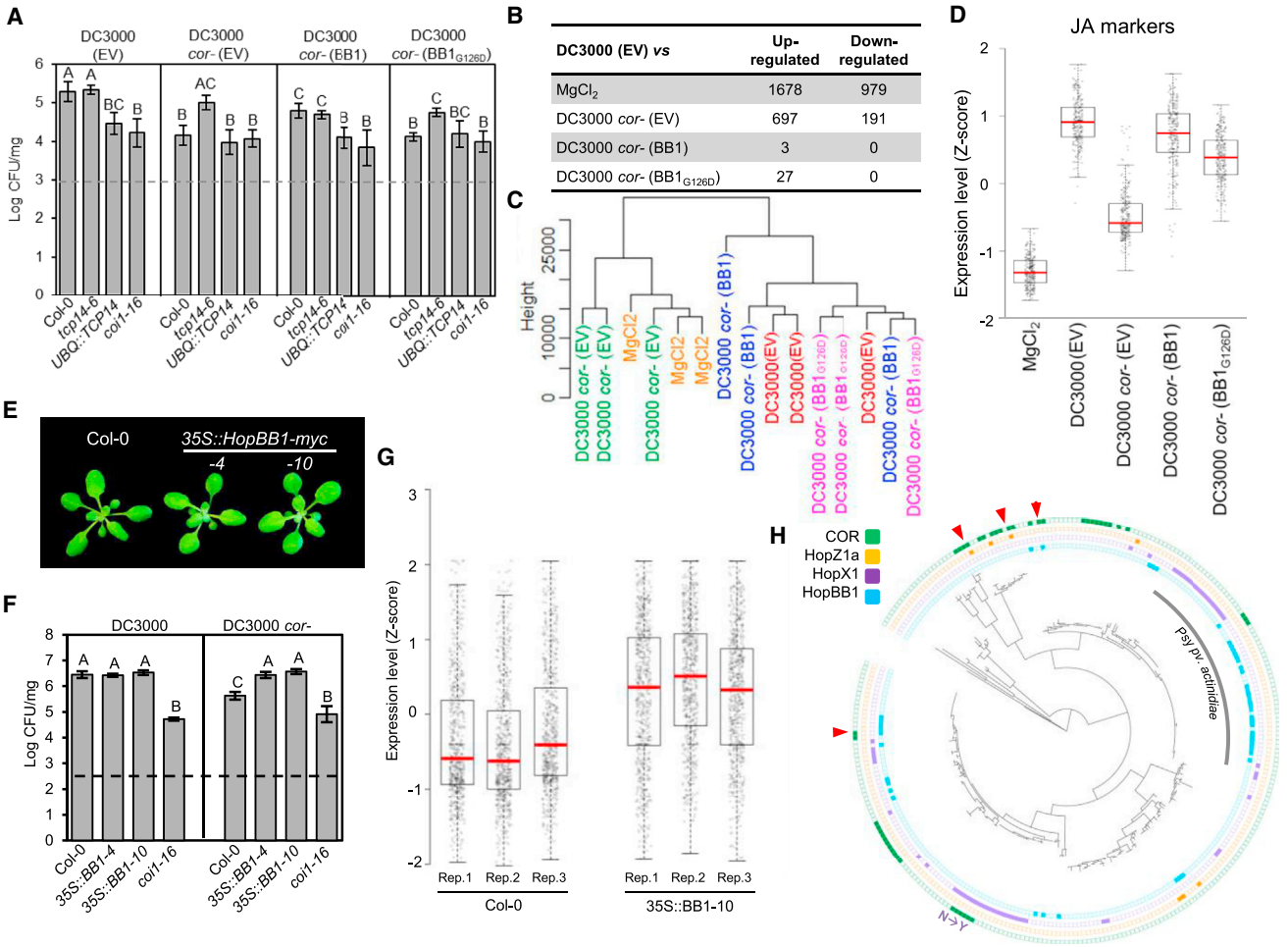


**Figure 3. HopBB1 Promotes Bacteria Growth and Activates JA Response**

(A) Bacterial-delivered HopBB1 promotes the growth of DC3000 *cor*− in Col-0. The 2-week-old plants were spray inoculated with a bacteria suspension at $OD_{600}$ = 0.2. CFU indicates bacterial colony formation units; error bars represent ± SD.

(B) Summary of transcriptional changes in Col-0 plants 24 hr after the treatment with DC3000 (EV), $MgCl_2$, and the coronatine-deficient mutant strains carrying the empty vector (EV), HopBB1, or $HopBB1_{G126D}$. Numbers represent the differentially expressed genes relative to the DC3000 treatment.

(C) Dendrogram constructed based on the entire transcriptome showing that the transcriptional signature of DC3000 *cor*− (EV)-treated plants resembles that of the mock treatment; DC3000 *cor*− expressing either HopBB1 or $HopBB1_{G126D}$ triggers similar transcriptional responses as DC3000 (EV).

(D) A set of 253 JA marker genes is activated by DC3000 (EV) and/or DC3000 *cor*− (HopBB1); $HopBB1_{G126D}$ has reduced ability to activate these genes.

(E) Transgenic *Arabidopsis* plants expressing HopBB1 are morphologically indistinguishable from Col-0 wild-type. Scale bar represents 5 mm.

(F) Plants expressing HopBB1 complement the growth defects of DC3000 *cor*−. Error bars represent ± SD.

(G) JA-responsive genes are activated in transgenic plants expressing HopBB1-myc. The Z-score-transformed expression of 672 JA-responsive marker genes is shown for three biological replicates of Col-0 and transgenic plants expressing HopBB1-myc.

(H) The distribution of HopBB1, HopX1, HopZ1a, and the coronatine biosynthesis pathway in 287 sequenced *P. syringae* genomes. Arrowhead indicates genomes containing two JA-activating tools; N→Y indicates that a polymorphism (N→Y) exists in the HopX1 allele.

See also Figure S3 and Tables S3 and S4.

in each lineage (Figure 3H; Table S5). This is particularly true across otherwise very closely related strains from the *Psy* pathovar *actinidae,* currently responsible for epidemic disease outbreaks that threaten the kiwi industries of New Zealand and Italy (Table S5; McCann et al., 2013).

## HopBB1-Mediated Degradation of TCP14 Requires $SCF^{COI1}$

Given that HopBB1 interacts with TCP14 and de-represses JA responses during infection, we investigated how HopBB1 disrupts TCP14 function. Delivery of native levels of HopBB1, but not $HopBB1_{G126D}$, led to reduced TCP14 protein accumulation (Figure 4A). MeJA treatment alone did not alter the accumulation of TCP14, indicating that the HopBB1-induced turnover of TCP14 was not a consequence of activated JA response (Figure 4B). TCP14 degradation in these experiments required the $SCF^{COI1}$ complex, since it was blocked in *coi1-1* plants expressing *UBQ::YFP-TCP14* (Figure 4C). Thus, HopBB1 promotes the degradation of TCP14 via the $SCF^{COI1}$ degradation pathway during infection, ultimately facilitating the activation of JA responses.

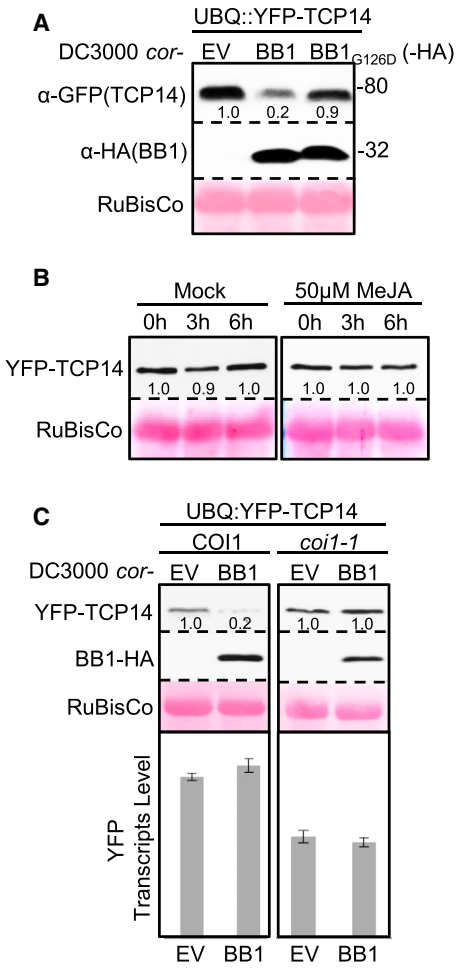


**Figure 4. HopBB1-Mediated Degradation of TCP14 Requires SCF$^{COI1}$ Pathway**

(A) Bacterial-delivered HopBB1, but not HopBB1$_{G126D}$, induced turnover of TCP14 during infection on *Arabidopsis*. Bacteria were hand-inoculated into leaves of 4-week-old plants at an $OD_{600}$ = 0.05. Samples were harvested 24 hr after inoculation.

(B) YFP-TCP14 is not subject to JA-mediated degradation in the absence of HopBB1 in *Arabidopsis*. The 2-week-old seedlings expressing *UBQ::YFP-TCP14* were sprayed with mock or 50 μM MeJA solution and sampled at the indicated time. Each sample was pooled from eight seedlings.

(C) *Pto*-delivered HopBB1 reduces TCP14 protein level in wild-type Col-0, but not in *coi1-1* mutant. Experiments were performed as Figure 4A. *YFP-TCP14* transcripts were quantified using real-time PCR. Error bars indicate ± SD.

## HopBB1 Interacts with JAZ3

We sought to define which component(s) of the SCF$^{COI1}$ pathway mediated TCP14 degradation. We confirmed the finding that JAZ3 interacted with HopBB1 (Mukhtar et al., 2011; Weßling et al., 2014; Figure S4A). Conditionally expressed HopBB1 co-immunoprecipitated JAZ3 in both transgenic *Arabidopsis* and transiently expressing *N. benthamiana* leaves (Figures 5A and S4D). HopBB1$_{111-283}$ was also sufficient for association with JAZ3 (Figure 5B). However, HopBB1$_{G126D}$ retained interaction with JAZ3 (Figures S4C and S4D), suggesting that a different association surface within the HopBB1 C terminus is required. JAZ3$_{208-297}$ is required for HopBB1 interaction, which is supported by association analyses in yeast and *N. benthamiana* (Figures 5C and 5D).

In contrast to HopX1 and HopZ1a, HopBB1 expression was not sufficient to alter JAZ3 accumulation (Figure S4E; Gimenez-Ibanez et al., 2014; Jiang et al., 2013). However, increasing HopBB1 levels did reduce the amount of MYC2 associated with JAZ3 in a competitive co-immunoprecipitation assay in *N. benthamiana*, indicating that HopBB1 interferes with the interaction of MYC2 and JAZ3 (Figure 5E). We developed a bimolecular fluorescence complementation (BiFC)-based assay to examine this disassociation in vivo. We co-infiltrated Agrobacterium strains carrying either a BiFC construct expressing JAZ3-nYFP, cYFP-MYC2, and mRFP as a co-expression reporter or a second construct carrying an estradiol-inducible HopBB1-CFP to test the ability of HopBB1 co-expression to block JAZ3-MYC2-interaction-mediated YFP reconstruction (Figures 5F, S4F, and S4G). Co-expression of HopBB1-CFP or HopBB1$_{G126D}$-CFP dramatically reduced the percentage of reconstituted YFP signal in CFP-and RFP-positive nuclei. Neither CFP nor CFP tagged with HaRxL45 (an *Hpa* effector that interacts with TCP14, but not JAZ3) (Weßling et al., 2014) altered the BiFC efficiency (Figures 5F and S4H). These observations support our contention that HopBB1-JAZ3 association interferes with the interaction between JAZ3 and MYC2 in vivo.

## TCP14 Is Subject to JA-Mediated Degradation in the Presence of HopBB1 and JAZ3

Since JAZ proteins are subject to SCF$^{COI1}$-mediated degradation, we tested how HopBB1 and JAZ3 influence the degradation of TCP14 in a reconstructed degradation system in *N. benthamiana*. TCP14 was not subject to JA-mediated protein degradation when transiently expressed (Figures 4B and6B) or when co-expressed with either HopBB1 or JAZ3 (Figures 6A and 6B). Importantly, when TCP14, JAZ3, and HopBB1 were co-expressed, levels of all three proteins were dramatically reduced upon MeJA treatment (Figure 6B). As anticipated, MYC2 levels were not reduced in these experiments (Figure 6C). Thus, HopBB1-mediated TCP14 turnover requires JA and JAZ3.

The protease inhibitor MG132 can block JA-triggered degradation of JAZ proteins (Chini et al., 2007; Thines et al., 2007); it also blocked HopBB1-mediated degradation of TCP14 (Figure 6D). We generated JAZ3$_{P302A\ R305A}$, an allele that cannot interact with COI1 and is thus MeJA resistant (Figures 6E, S5A, and S5B). Importantly, JAZ3$_{P302A\ R305A}$ still interacted with HopBB1 in yeast, suggesting that its overall structure is not altered (Figure S5C). When we co-expressed JAZ3$_{P302A\ R305A}$ with TCP14 and HopBB1, MeJA-induced degradation of HopBB1 and TCP14 was blocked (Figure 6E). This observation suggested that SCF$^{COI1}$-dependent degradation of JAZ3 is required for HopBB1-mediated, JA-dependent turnover of TCP14. TCP14 turnover was not driven by HaRxL45 co-expression in the presence of JAZ3 (Figure 6F), implying that effectors interacting with TCP14 modulate its activity by at least two different mechanisms. Remarkably, HopBB1$_{G126D}$ failed to mediate TCP14 turnover but was still degraded with JAZ3 in the presence of MeJA (Figure 6G). Conversely, the TCP14$_{RSAAST/NAAIRS}$ mutant that fails to interact with HopBB1 was also resistant to HopBB1-mediated degradation (Figure 6H). Thus, HopBB1-mediated degradation of

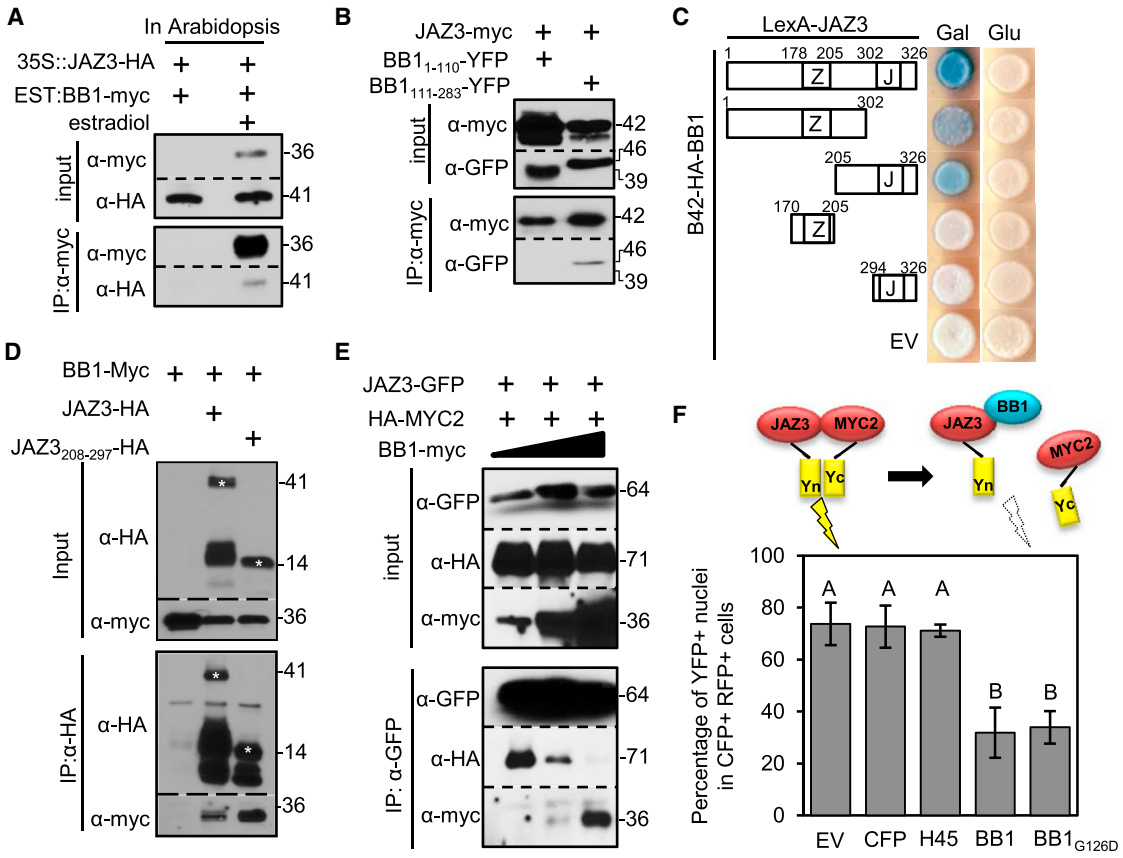


**Figure 5. HopBB1 Interacts with JAZ3 and Disrupts Its Association with MYC2**

(A) HopBB1 interacts with JAZ3 in *Arabidopsis*. HopBB1-myc conditionally expressed from an estradiol-inducible promoter was transformed into *Arabidopsis* constitutively expressing JAZ3-HA from a 35S promoter. The 3-week-old seedlings were induced with 50 μM estradiol and sampled 6 hr after induction.

(B) The C terminus (111–283) of HopBB1 is sufficient to associate with JAZ3 in *N. benthamiana*.

(C) HopBB1 interacts with an uncharacterized JAZ3 domain (206–302) in yeast.

(D) HopBB1 associates with an uncharacterized JAZ3 domain (206–302) in *N. benthamiana*.

(E) HopBB1 reduces the association between JAZ3 and MYC2 in planta. Proteins were transiently co-expressed in *N. benthamiana*. HopBB1 was induced using a gradient of estradiol (0.01 μM, 1 μM, and 10 μM) 6 hr after Agrobacteria infiltration. Samples were harvested 18 hr after induction.

(F) HopBB1 disrupts the BiFC signal generated from the association between JAZ3 and MYC2. The co-expression of HopBB1 or HopBB1$_{G126D}$ reduces the efficiency from 80% to 20%. RFP-positive cells were examined for the presence of CFP and YFP signal in nuclei. For each combination, the ratios were calculated by counting approximately 200 nuclei collected from four independent samples. Error bars indicate ± SD.

See also Figure S4.

TCP14 requires its interactions with TCP14 and the degradation of JAZ3 through SCF$^{COI1}$.

## HopBB1 Recruits TCP14 into a JAZ3-Containing Sub-nuclear Structure

We previously demonstrated that TCP14 re-locates HopBB1 into an uncharacterized sub-nuclear structure (Figures 7A and 7B, top, and S6A; Weßling et al., 2014). Similarly, we noted that JAZ3 also forms sub-nuclear foci (Figure 7A). We found that HopBB1 can also be re-localized into JAZ3 foci (Figures 7B, middle, and S6B). Strikingly, JAZ3 foci and TCP14 foci did not overlap when co-expressed, implying that they represent different structures (Figures 7B, bottom, and S6C). We then co-expressed a CFP-tagged HopBB1 together with TCP14 and JAZ3. In nuclei with HopBB1-CFP (but not with CFP alone), the CFP, YFP, and RFP signals co-localized in the same foci (Figures 7C and S6D), suggesting that HopBB1 re-distributed TCP14 and JAZ3 from separate sub-nuclear foci into the same structure. Although HopBB1$_{G126D}$ failed to associate with TCP14 in both Y2H and co-IP assay, it was still re-localized by TCP14, suggesting that these assays report different interaction affinities (Figure S6E). For this reason, we could not specifically test the requirement of HopBB1-TCP14 interaction in re-distributing JAZ3 and TCP14. However, TCP14$_{RSAAST/NAAIRS}$, which still forms nuclear foci but cannot interact with HopBB1, also cannot be fully re-distributed to the JAZ3-containing foci in the presence of HopBB1 (Figure 7D). This result confirms that re-distribution of TCP14 to JAZ3-containing foci requires its association with HopBB1.

We utilized TCP14 and JAZ3 mutants to examine functional requirements for the formation of sub-nuclear foci. Amino acids H121, R130, and L161 in the TCP domain are conserved in all 24 *Arabidopsis* TCP proteins (Figure S6F). Single mutation in any of these abolished TCP4 binding to DNA (Aggarwal et al.,

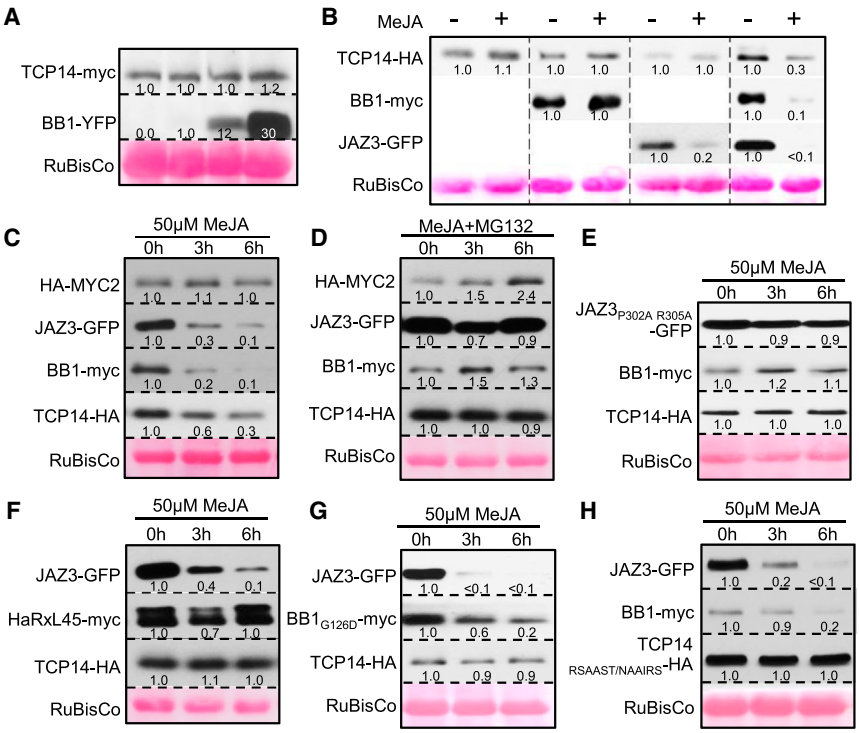


**Figure 6. TCP14 Is Subject to JA-Mediated Degradation in the Presence of HopBB1 and JAZ3**

(A) HopBB1 alone does not trigger TCP14 degradation without MeJA. Leaves were co-infiltrated with Agrobacteria delivering 35S::TCP14-myc or EST::HopBB1-YFP-HA genes.

(B) TCP14 is subject to JA-mediated degradation in the presence of HopBB1 and JAZ3. Agrobacteria carrying vectors expressing each protein under 35S constitutive promoter were co-infiltrated into *N. benthamiana* leaves. A total of 50 μM of MeJA was hand-infiltrated into leaves 24 hr after inoculation. Numbers below western signal indicate the relative signal intensity. The same method was applied to (B)–(H).

(C) MYC2 is not co-degraded with TCP14.

(D) HopBB1-mediated degradation of TCP14 is blocked by the 26S proteasome inhibitor MG132. Totals of 50 μM MeJA and 50 μM MG132 were co-infiltrated 24 hr after inoculation.

(E) The recruitment of JAZ3 to $SCF^{COI1}$ is required for HopBB1-mediated degradation of TCP14.

(F) HaRxL45 cannot mediate TCP14 degradation with the presence of JAZ3 and MeJA.

(G) $HopBB1_{G126D}$ cannot mediate TCP14 degradation with the presence of JAZ3 and MeJA.

(H) $TCP14_{RSAAST/NAAIRS}$ is not subject to HopBB1-mediated degradation.

See also Figure S5.

2010). $TCP14_{H121Q\ R130K\ L161N}$ almost completely abolished the formation of sub-nuclear foci in transgenic *Arabidopsis*, although it was still exclusively localized in nuclei and retained its ability to homodimerize and associate with HopBB1 (Figures 7E and S6G–S6I). Thus, the formation of the TCP14 nuclear foci is dependent on TCP14 DNA binding activity.

We tested whether the JAZ3 nuclear foci represent a structure for its degradation. We observed that JAZ3-RFP formed sub-nuclear foci in Col-0, but not in *coi1-1* (Figure 7F), a COI1 allele without detectable protein accumulation (He et al., 2012). $JAZ3_{P302A\ R305A}$ was unable to form nuclear foci (Figure 7G). Thus, formation of JAZ3 nuclear foci requires COI1. Importantly, $JAZ3_{P302A\ R305A}$ was re-localized into TCP14 sub-nuclear foci only in the presence of HopBB1 (Figures 7H and 7I). In sum, these data are consistent with a model wherein HopBB1 links template DNA-bound TCP14 to a degradation complex containing JAZ3.

## DISCUSSION

We demonstrate that the HopBB1 type III effector protein modulates subsets of two *Arabidopsis* transcriptional regulons—those negatively regulated by TCP14 and activated by MYC2—leading to a fine-tuned perturbation in plant defense output that facilitates bacterial pathogen proliferation. Expressing HopBB1 from bacteria or in *Arabidopsis* rescues the virulence defect of a pathogenic *Psy* strain lacking the JA-Ile structural mimic, coronatine, suggesting its role as a regulator of host JA response (Figure 3). HopBB1 has dual functions in de-repressing the JA signaling pathway: it facilitates the degradation of TCP14 and possibly other TCPs through $SCF^{COI1}$ by connecting JAZ3 to it (Figures 4, 6, and 7), and it disrupts the inhibitory association between JAZ3 and MYC2, leading to MYC2-dependent transcriptional activation of JA responses (Figure 5), which may contribute to the residual function of $HopBB1_{G126D}$ in activating JA response (Figure 3D). However, only subsets of either the TCP14 or MYC regulons are transcriptionally perturbed in the presence of HopBB1 (Figures 1D and S3E). Thus, we propose that HopBB1 has evolved to minimize pleiotropic negative effects on host physiology generated by wholesale de-repression of the JA response output (defined here by MeJA treatment) while maintaining the ability to modulate defense hormone signaling to the pathogen's advantage.

Four *Psy* virulence factors—coronatine, HopX1, HopZ1a and HopBB1—activate the JA response at different steps in the signaling pathway. Coronatine and HopX1 stimulate an overlapping spectrum of JA-related phenotypes, including activation of a few tested JA-responsive genes, promotion of stomatal opening, and induction of chlorotic symptoms in infected plants. This pleiotropy is likely attributable to the ability of HopX1 to directly cleave almost all members of the JAZ family; this is functionally analogous to coronatine action (Gimenez-Ibanez et al., 2014; Kloek et al., 2001). In contrast, we conclude that HopBB1 expression specifically activates a subset of JA-mediated responses (Figures 3D and S3E). This conclusion is supported by several observations. First, expressing HopBB1 in *Arabidopsis* activates only about 18% (168 of 933) of JA-responsive genes (Figure S3E). Second, HopBB1 manipulates JA response by dissociating the JAZ3-MYC2 complex, leading to $SCF^{COI1}$-dependent degradation of the JAZ3-HopBB1-TCP14 complex (Figures 6 and 7). Third, HopBB1 is apparently more selective than HopX1 or the action of coronatine, since it only interacts with a small subset of JAZ proteins and TCP14 to pinpoint a sector of JA regulon. Fourth, the chlorotic phenotypes observed

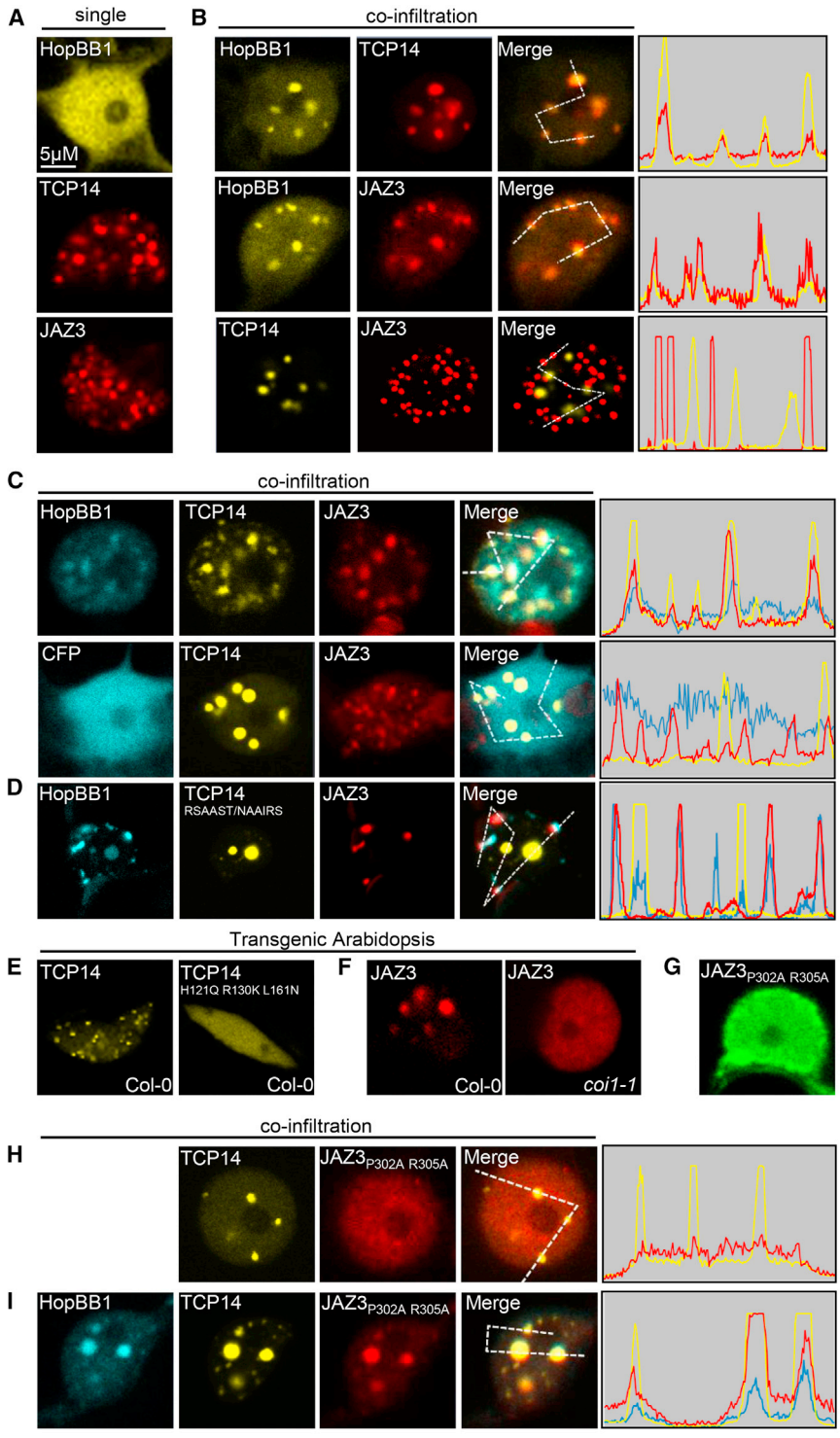


**Figure 7. HopBB1 Recruits TCP14 to a JAZ3-Containing Degradation Site**

(A) Localization of HopBB1, TCP14, and JAZ3 in nuclei. HopBB1 is evenly distributed in nuclei, while TCP14 and JAZ3 form sub-nuclear foci. Scale bar represents 5 μM. Proteins were transiently expressed in *N. benthamiana* for (A)–(D) and (G)–(I).

(B) HopBB1 was re-localized to sub-nuclear foci by TCP14 (top) and JAZ3 (middle). However, TCP14 and JAZ3 localize in distinct nuclear foci (bottom). Histograms represent the intensity of fluorescent signal on the pathway of the lines in the "Merged" panel.

(C) HopBB1 (top), but not CFP (bottom), drives TCP14 and JAZ3 into the same sub-nuclear foci.

(D) HopBB1 cannot co-localize $TCP14_{RSAAST/NAAIRS}$-YFP into the same foci as JAZ3-RFP.

(E) The formation of TCP14 foci depends on TCP14's binding DNA ability. YFP-TCP14, but not $TCP14_{H121Q\ R130K\ L161N}$, expressed under UBQ promoter forms sub-nuclear foci in transgenic *Arabidopsis*.

(F) The formation of JAZ3 foci depends on JAZ3's ability to associate with COI1. JAZ3-RFP expressed from a constitutive 35S promoter forms sub-nuclear foci in transgenic *Arabidopsis* Col-0, but not in *coi1-1* mutant. Images in (E) and (F) were taken from cotyledon epidermal cells in transgenic *Arabidopsis*.

(G) $JAZ3_{P302A\ R305A}$ cannot form sub-nuclear foci in *N. benthamiana*.

(H) TCP14 cannot re-localize $JAZ3_{P302A\ R305A}$.

(I) TCP14 re-located $JAZ3_{P302A\ R305A}$ to nuclear foci in the presence of HopBB1.

See also Figure S6.

in HopX1 transgenic plants and coronatine-treated plants are not visible following either constitutive or conditional expression of HopBB1 (Figures 3E and S3F). Importantly, coronatine-induced chlorosis can be de-coupled from bacterial growth promotion and repression of SA-dependent responses (Kloek et al., 2001). We suggest that HopBB1 fine-tunes JA response by targeting a sub-group of JAZ proteins, leading to transcriptional activation of genes enriched in those co-regulated by TCP and MYC.

Modulation of plant JA responses is an important virulence strategy for phytopathogenic bacteria (Gimenez-Ibanez et al., 2014; Jiang et al., 2013; Zheng et al., 2012). The evolutionary mechanism driving the mutual exclusivity of JA-modulating virulence factors in *Psy* genomes (Figure 3H and Table S5) is unknown, but is consistent with negative frequency-dependent selection driven by the centrality of JA response manipulation to *Psy* virulence, balanced by host immune recognition. This particular arms race is evident in various plants. The ZAR1 NLR innate immune receptor in *Arabidopsis* recognizes the acetylation activity of HopZ1a on the ZED1 pseudokinase (Lewis et al., 2013). Alleles of HopX are recognized by the as-yet-uncloned *R2* disease-resistance gene in beans (Mansfield et al., 1994). Additionally, plants can evolve JAZ proteins that are resistant to COI1-mediated degradation (Chung and Howe, 2009; Shyu et al., 2012). These JAZ proteins might antagonize coronatine function. Although a host surveillance mechanism recognizing

HopBB1 has not been discovered, it could be achieved by monitoring an as-yet-unknown activity on TCP14 or JAZ3, or on the relevant interacting domains integrated into recently described decoy fusion NLR proteins (Cesari et al., 2014).

TCP14 is targeted by effectors from three evolutionarily divergent pathogens (Weßling et al., 2014). Our results demonstrated that TCP14 contributes to disease resistance against *Psy* as a negative regulator of JA signaling (Figure 1). JA-responsive genes are repressed in seedlings overexpressing TCP14 (Figure 1D), and *tcp14* mutants rescue the growth defects of DC3000 *cor*− (Figure 1C). However, TCP14 may regulate other defense pathways against different pathogens at different developmental stages or in different tissues. Indeed, Kim et al. (2014) suggested that TCP8, TCP14 and TCP15 are part of a transcriptional complex involved in NLR-mediated immune system signaling. Thus, we speculate that the TCP14-interacting effectors identified from *Psy*, *Hpa*, and *Go* will manipulate TCP14 via different mechanisms to facilitate proliferation of pathogens with different life cycles and infection strategies. It is therefore noteworthy that an *Hpa*-derived TCP14-interacting effector, HaRxL45, fails to activate degradation of TCP14 in the presence of JA, indicating that this effector modulates TCP14 in a manner mechanistically different from that of HopBB1. Future studies will explore the different sectors of the immune response that are under direct control of TCP14.

## EXPERIMENTAL PROCEDURES

### Transient Protein Expression in *N. benthamiana*

*N. benthamiana* plants were grown at 24°C (day) and 20°C (night) under a 16-hr light and 8-hr dark cycle. Agrobacteria were collected and re-suspended in 2 mL re-suspension buffer (10 mM MES [pH 5.6], 10 mM $MgCl_2$, and 200 μM acetosyringone) to a final concentration of $OD_{600}$ = 0.2. To reach equal protein accumulation, the final concentration of agrobacteria expressing HopBB1 and $HopBB1_{G126D}$ was $OD_{600}$ (0.02) and $OD_{600}$ (0.2), respectively. GV3101 carrying 35S promoter-driven p19 protein was co-infiltrated at $OD_{600}$ = 0.05 in each experiment to prevent the onset of post-transcriptional gene silencing and improve the efficiency of transient expression. *Agrobacterium tumefaciens* GV3101 (pMP90) transformed with mixtures of binary vector constructs were infiltrated into *N. benthamiana* leaves using a needleless syringe. Samples were harvested 24 hr after infiltration unless otherwise indicated.

### Immunoblot and Co-immunoprecipitation Analyses

Leaf tissues were ground in liquid nitrogen and extracted with 150–200 μL of grinding buffer (50 mM Tris [pH8.0], 1% SDS, 1 mM EDTA) also containing 1 uL/mL β-mercaptoethanol and 1× protease inhibitor (Sigma-Aldrich). The lysates were centrifuged at 12,000 rpm for 10 min at 4°C. Supernatants were collected, and the protein concentration was determined with the BioRad Bradford quantification method (BioRad).

For co-immunoprecipitation analyses, proteins were extracted from 0.5 g of fresh tissue using 2 mL extraction buffer (50 mM HEPES [pH 7.5], 50 mM NaCl, 10 mM EDTA [pH 8.0], 0.5% Triton X-100, 5 mM DTT, and 1× Plant protease inhibitor cocktail from Sigma-Aldrich). Magnetic labeling and separation of tagged proteins was performed using mMACS Epitope Tag Protein Isolation Kit (Miltenyi Biotec). Protein samples were separated by SDS-PAGE. Immunoblots were performed with a 1:1,000 dilution of α-HA (Roche), 1:1,000 dilution of α-GFP (Roche), 1:1,000 dilution of α-myc, and 1:1,000 dilution of α-FLAG. Blots were detected by ECL prime (GE Healthcare).

### Mutagenesis

$JAZ3_{P302A\ R305A}$ and $TCP14_{H121Q\ R130K\ L161N}$ were generated using the QuikChange Lightning Site-Directed Mutagenesis Kit (Agilent). Random mutagenesis of HopBB1 was performed using the GeneMorph II EZClone Domain Mutagenesis Kit. A pJG4-5-HopBB1 construct was mutagenized according to the manufacture's protocol. The library was transformed into yeast strain RFY206. Each RFY206 (pJG4-5-HopBB1) clone was mated with yeast EGY48 strain carrying pEG202-TCP14 or pEG202-JAZ3. HopBB1 clones that lost interaction with either TCP14 or JAZ3, but not both, were sequenced. If multiple mutations were present in one clone, single mutations were introduced into wild-type HopBB1 and confirmed by re-testing.

### Real-Time PCR

Total RNAs were extracted with the RNeasy Plant Mini kit (QIAGEN). cDNAs were synthesized using SuperScript III Reverse Transcriptase (Invitrogen). qPCR was performed using SYBR green master mix (Applied Biosystems) with the following cycle: 95°C for 3min, 40 cycles of 95°C for 15 s, 58°C for 15 s, and 72°C for 20 s. Expression levels were normalized to multiple endogenous controls including UBQ5 (AT3G62250), TUB (AT5G62690), and SAND (AT2G28390).

### Statistics for In Planta Bacterial Growth

In Figures 1C, 3A, and3F, error bars represent ± SD. Statistics were performed using one-way ANOVA test with Tukey-Kramer HSD with 95% confidence. In each case, the result displayed is one of three independent analyses giving similar results.

## ACCESSION NUMBERS

The NCBI Gene Expression Omnibus accession number for the RNA-seq data reported in this paper is GEO: GSE90606.

## SUPPLEMENTAL INFORMATION

Supplemental Information includes Supplemental Experimental Procedures, six figures, and six tables and can be found with this article online at http://dx.doi.org/10.1016/j.chom.2017.01.003.

## AUTHOR CONTRIBUTIONS

L.Y., P.J.P.L.T., P.E., and J.L.D. designed the study. L.Y., P.J.P.L.T., P.E., S.B., Y.H., I.S.-G., O.M.F., M.E.E., and P.M. performed experiments. L.Y., P.J.P.L.T., and J.L.D. wrote the paper with input from other authors.

## ACKNOWLEDGMENTS

We thank Dangl-Grant lab members for fruitful discussions and criticisms, Drs. Freddy Monteiro and Farid El Kasmi for tissue harvest, the UNC-CH High Throughput Sequencing Center for assistance, and Prof. Sarah Grant for critical comments on the manuscript. We thank Prof. Sheng Yang He of Michigan State University for the gift of JAZ3 fragments, entry clones of JAZ family members, and 35S::JAZ3-HA plants, and we thank Prof. Steve A. Kay for entry clones of TCP family members. This work was funded by grants to J.L.D. from the National Institutes of Health (1RO1 GM107444), the Gordon and Betty Moore Foundation (GBMF3030), and the HHMI. J.L.D. is an Investigator of the Howard Hughes Medical Institute. L.Y. was funded in part by the Gordon and Betty Moore Foundation through grant GBMF 2550.02 to the Life Sciences Research Foundation. P.J.P.L.T. was supported in part by a fellowship from the Pew Latin American Fellows Program in the Biomedical Sciences (00026198). Y.H. was supported by a Distinguished Guest Professorship, Eberhard-Karls-Universität, Tübingen, Germany to J.L.D. O.M.F. is supported by National Institutes of Health grant F32 GM117758-01.

Received: September 25, 2016
Revised: November 2, 2016
Accepted: December 19, 2016
Published: January 26, 2017

## REFERENCES

Aggarwal, P., Das Gupta, M., Joseph, A.P., Chatterjee, N., Srinivasan, N., and Nath, U. (2010). Identification of specific DNA binding residues in the TCP family of transcription factors in Arabidopsis. Plant Cell *22*, 1174–1189.

Belkhadir, Y., Yang, L., Hetzel, J., Dangl, J.L., and Chory, J. (2014). The growth-defense pivot: crisis management in plants mediated by LRR-RK surface receptors. Trends Biochem. Sci. *39*, 447–456.

Bentham, A., Burdett, H., Anderson, P.A., Williams, S.J., and Kobe, B. (2016). Animal NLRs provide structural insights into plant NLR function. Ann. Bot. (Lond.). Published online August 25, 2016. http://dx.doi.org/10.1093/aob/mcw171.

Browse, J. (2009). Jasmonate passes muster: a receptor and targets for the defense hormone. Annu. Rev. Plant Biol. *60*, 183–205.

Cesari, S., Bernoux, M., Moncuquet, P., Kroj, T., and Dodds, P.N. (2014). A novel conserved mechanism for plant NLR protein pairs: the "integrated decoy" hypothesis. Front. Plant Sci. *5*, 606.

Chini, A., Fonseca, S., Fernández, G., Adie, B., Chico, J.M., Lorenzo, O., García-Casado, G., López-Vidriero, I., Lozano, F.M., Ponce, M.R., et al. (2007). The JAZ family of repressors is the missing link in jasmonate signalling. Nature *448*, 666–671.

Chung, H.S., and Howe, G.A. (2009). A critical role for the TIFY motif in repression of jasmonate signaling by a stabilized splice variant of the JASMONATE ZIM-domain protein JAZ10 in Arabidopsis. Plant Cell *21*, 131–145.

Dreze, M., Carvunis, A.-R., Charloteaux, B., Galli, M., Pevzner, S.J., Tasan, M., Ahn, Y.-Y., Balumuri, P., Barabási, A.-L., and Bautista, V.; Arabidopsis Interactome Mapping Consortium (2011). Evidence for network evolution in an Arabidopsis interactome map. Science *333*, 601–607.

Franco-Zorrilla, J.M., López-Vidriero, I., Carrasco, J.L., Godoy, M., Vera, P., and Solano, R. (2014). DNA-binding specificities of plant transcription factors and their potential to define target genes. Proc. Natl. Acad. Sci. USA *111*, 2367–2372.

Gimenez-Ibanez, S., Boter, M., Fernández-Barbero, G., Chini, A., Rathjen, J.P., and Solano, R. (2014). The bacterial effector HopX1 targets JAZ transcriptional repressors to activate jasmonate signaling and promote infection in Arabidopsis. PLoS Biol. *12*, e1001792.

He, P., Chintamanani, S., Chen, Z., Zhu, L., Kunkel, B.N., Alfano, J.R., Tang, X., and Zhou, J.M. (2004). Activation of a COI1-dependent pathway in Arabidopsis by Pseudomonas syringae type III effectors and coronatine. Plant J. *37*, 589–602.

He, Y., Chung, E.H., Hubert, D.A., Tornero, P., and Dangl, J.L. (2012). Specific missense alleles of the arabidopsis jasmonic acid co-receptor COI1 regulate innate immune receptor accumulation and function. PLoS Genet. *8*, e1003018.

Jiang, S., Yao, J., Ma, K.W., Zhou, H., Song, J., He, S.Y., and Ma, W. (2013). Bacterial effector activates jasmonate signaling by directly targeting JAZ transcriptional repressors. PLoS Pathog. *9*, e1003715.

Jones, J.D., and Dangl, J.L. (2006). The plant immune system. Nature *444*, 323–329.

Katsir, L., Schilmiller, A.L., Staswick, P.E., He, S.Y., and Howe, G.A. (2008). COI1 is a critical component of a receptor for jasmonate and the bacterial virulence factor coronatine. Proc. Natl. Acad. Sci. USA *105*, 7100–7105.

Kazan, K., and Lyons, R. (2014). Intervention of phytohormone pathways by pathogen effectors. Plant Cell *26*, 2285–2309.

Kazan, K., and Manners, J.M. (2013). MYC2: the master in action. Mol. Plant *6*, 686–703.

Kieffer, M., Master, V., Waites, R., and Davies, B. (2011). TCP14 and TCP15 affect internode length and leaf shape in Arabidopsis. Plant J. *68*, 147–158.

Kim, S.H., Son, G.H., Bhattacharjee, S., Kim, H.J., Nam, J.C., Nguyen, P.D.T., Hong, J.C., and Gassmann, W. (2014). The Arabidopsis immune adaptor SRFR1 interacts with TCP transcription factors that redundantly contribute to effector-triggered immunity. Plant J. *78*, 978–989.

Kloek, A.P., Verbsky, M.L., Sharma, S.B., Schoelz, J.E., Vogel, J., Klessig, D.F., and Kunkel, B.N. (2001). Resistance to Pseudomonas syringae conferred by an Arabidopsis thaliana coronatine-insensitive (coi1) mutation occurs through two distinct mechanisms. Plant J. *26*, 509–522.

Kosugi, S., and Ohashi, Y. (2002). DNA binding and dimerization specificity and potential targets for the TCP protein family. Plant J. *30*, 337–348.

Lewis, J.D., Lee, A.H., Hassan, J.A., Wan, J., Hurley, B., Jhingree, J.R., Wang, P.W., Lo, T., Youn, J.Y., Guttman, D.S., and Desveaux, D. (2013). The Arabidopsis ZED1 pseudokinase is required for ZAR1-mediated immunity induced by the Pseudomonas syringae type III effector HopZ1a. Proc. Natl. Acad. Sci. USA *110*, 18722–18727.

Lewis, L.A., Polanski, K., de Torres-Zabala, M., Jayaraman, S., Bowden, L., Moore, J., Penfold, C.A., Jenkins, D.J., Hill, C., Baxter, L., et al. (2015). Transcriptional dynamics driving MAMP-triggered immunity and pathogen effector-mediated immunosuppression in Arabidopsis leaves following infection with pseudomonas syringae pv tomato DC3000. Plant Cell *27*, 3038–3064.

Lopez, J.A., Sun, Y., Blair, P.B., and Mukhtar, M.S. (2015). TCP three-way handshake: linking developmental processes with plant immunity. Trends Plant Sci. *20*, 238–245.

Mansfield, J., Jenner, C., Hockenhull, R., Bennett, M.A., and Stewart, R. (1994). Characterization of avrPphE, a gene for cultivar-specific avirulence from Pseudomonas syringae pv. phaseolicola which is physically linked to hrpY, a new hrp gene identified in the halo-blight bacterium. Mol. Plant Microbe Interact. *7*, 726–739.

McCann, H.C., Rikkerink, E.H., Bertels, F., Fiers, M., Lu, A., Rees-George, J., Andersen, M.T., Gleave, A.P., Haubold, B., Wohlers, M.W., et al. (2013). Genomic analysis of the Kiwifruit pathogen Pseudomonas syringae pv. actinidiae provides insight into the origins of an emergent plant disease. PLoS Pathog. *9*, e1003503.

Mukhtar, M.S., Carvunis, A.R., Dreze, M., Epple, P., Steinbrenner, J., Moore, J., Tasan, M., Galli, M., Hao, T., Nishimura, M.T., et al.; European Union Effectoromics Consortium (2011). Independently evolved virulence effectors converge onto hubs in a plant immune system network. Science *333*, 596–601.

Nimchuk, Z.L., Fisher, E.J., Desveaux, D., Chang, J.H., and Dangl, J.L. (2007). The HopX (AvrPphE) family of Pseudomonas syringae type III effectors require a catalytic triad and a novel N-terminal domain for function. Mol. Plant Microbe Interact. *20*, 346–357.

Pauwels, L., Barbero, G.F., Geerinck, J., Tilleman, S., Grunewald, W., Pérez, A.C., Chico, J.M., Bossche, R.V., Sewell, J., Gil, E., et al. (2010). NINJA connects the co-repressor TOPLESS to jasmonate signalling. Nature *464*, 788–791.

Qi, T., Wang, J., Huang, H., Liu, B., Gao, H., Liu, Y., Song, S., and Xie, D. (2015). Regulation of Jasmonate-Induced Leaf Senescence by Antagonism between bHLH Subgroup IIIe and IIId Factors in Arabidopsis. Plant Cell *27*, 1634–1649.

Resentini, F., Felipo-Benavent, A., Colombo, L., Blázquez, M.A., Alabadí, D., and Masiero, S. (2015). TCP14 and TCP15 mediate the promotion of seed germination by gibberellins in Arabidopsis thaliana. Mol. Plant *8*, 482–485.

Robert-Seilaniantz, A., Grant, M., and Jones, J.D. (2011). Hormone crosstalk in plant disease and defense: more than just jasmonate-salicylate antagonism. Annu. Rev. Phytopathol. *49*, 317–343.

Schmelz, E.A., Engelberth, J., Alborn, H.T., O'Donnell, P., Sammons, M., Toshima, H., and Tumlinson, J.H., 3rd (2003). Simultaneous analysis of phytohormones, phytotoxins, and volatile organic compounds in plants. Proc. Natl. Acad. Sci. USA *100*, 10552–10557.

Sheard, L.B., Tan, X., Mao, H., Withers, J., Ben-Nissan, G., Hinds, T.R., Kobayashi, Y., Hsu, F.F., Sharon, M., Browse, J., et al. (2010). Jasmonate perception by inositol-phosphate-potentiated COI1-JAZ co-receptor. Nature *468*, 400–405.

Shyu, C., Figueroa, P., Depew, C.L., Cooke, T.F., Sheard, L.B., Moreno, J.E., Katsir, L., Zheng, N., Browse, J., and Howe, G.A. (2012). JAZ8 lacks a canonical degron and has an EAR motif that mediates transcriptional repression of jasmonate responses in Arabidopsis. Plant Cell *24*, 536–550.

Steiner, E., Efroni, I., Gopalraj, M., Saathoff, K., Tseng, T.S., Kieffer, M., Eshed, Y., Olszewski, N., and Weiss, D. (2012). The Arabidopsis O-linked N-acetylglucosamine transferase SPINDLY interacts with class I TCPs to facilitate cytokinin responses in leaves and flowers. Plant Cell *24*, 96–108.

Sugio, A., Kingdom, H.N., MacLean, A.M., Grieve, V.M., and Hogenhout, S.A. (2011). Phytoplasma protein effector SAP11 enhances insect vector reproduction by manipulating plant development and defense hormone biosynthesis. Proc. Natl. Acad. Sci. USA *108*, E1254–E1263.

Thines, B., Katsir, L., Melotto, M., Niu, Y., Mandaokar, A., Liu, G., Nomura, K., He, S.Y., Howe, G.A., and Browse, J. (2007). JAZ repressor proteins are

targets of the SCF(COI1) complex during jasmonate signalling. Nature *448*, 661–665.

van der Hoorn, R.A., and Kamoun, S. (2008). From Guard to Decoy: a new model for perception of plant pathogen effectors. Plant Cell *20*, 2009–2017.

Wasternack, C., and Hause, B. (2013). Jasmonates: biosynthesis, perception, signal transduction and action in plant stress response, growth and development. An update to the 2007 review in Annals of Botany. Ann. Bot. (Lond.) *111*, 1021–1058.

Weßling, R., Epple, P., Altmann, S., He, Y., Yang, L., Henz, S.R., McDonald, N., Wiley, K., Bader, K.C., Gläßer, C., et al. (2014). Convergent targeting of a common host protein-network by pathogen effectors from three kingdoms of life. Cell Host Microbe *16*, 364–375.

Wilson, I.A., Haft, D.H., Getzoff, E.D., Tainer, J.A., Lerner, R.A., and Brenner, S. (1985). Identical short peptide sequences in unrelated proteins can have different conformations: a testing ground for theories of immune recognition. Proc. Natl. Acad. Sci. USA *82*, 5255–5259.

Zhang, F., Yao, J., Ke, J., Zhang, L., Lam, V.Q., Xin, X.F., Zhou, X.E., Chen, J., Brunzelle, J., Griffin, P.R., et al. (2015). Structural basis of JAZ repression of MYC transcription factors in jasmonate signalling. Nature *525*, 269–273.

Zheng, X.Y., Spivey, N.W., Zeng, W., Liu, P.P., Fu, Z.Q., Klessig, D.F., He, S.Y., and Dong, X. (2012). Coronatine promotes Pseudomonas syringae virulence in plants by activating a signaling cascade that inhibits salicylic acid accumulation. Cell Host Microbe *11*, 587–596.

**Cell Host & Microbe, Volume *21***

## Supplemental Information

# *Pseudomonas syringae* Type III Effector HopBB1 Promotes Host Transcriptional Repressor Degradation to Regulate Phytohormone Responses and Virulence

**Li Yang, Paulo José Pereira Lima Teixeira, Surojit Biswas, Omri M. Finkel, Yijian He, Isai Salas-Gonzalez, Marie E. English, Petra Epple, Piotr Mieczkowski, and Jeffery L. Dangl**

# sFigure 1

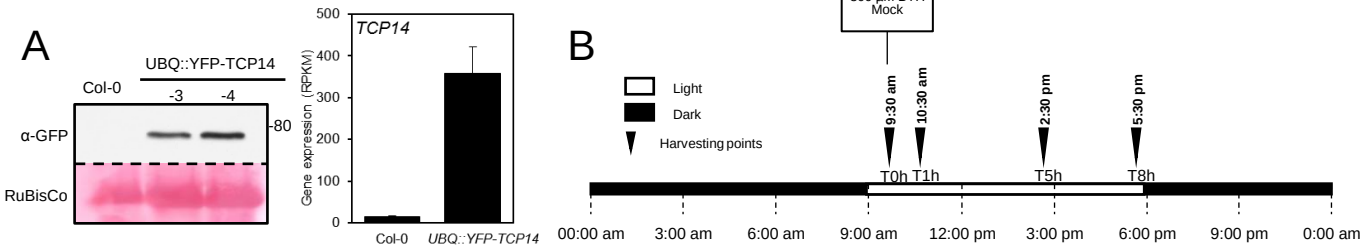


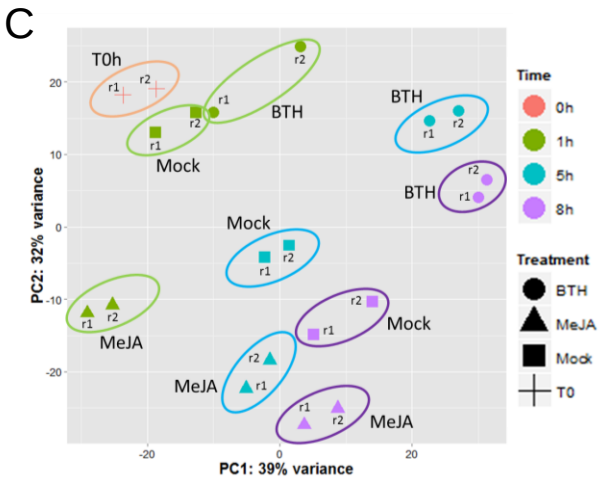


D

| | Up-regulated | Down-regulated |
|---|---|---|
| MeJA | 933 | 1054 |
| BTH | 2357 | 1593 |

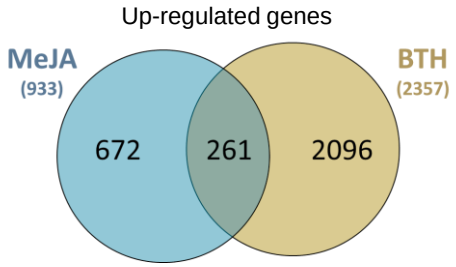


E

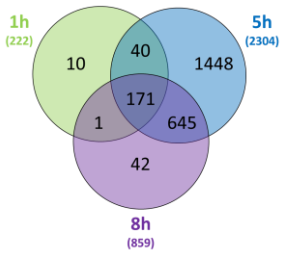


Top10 enriched GO terms

| Gene Set Name(NO. Genes) | FDR |
|---|---|
| DEFENSE_RESPONSE(1644) | 9.67E-158 |
| RESPONSE_TO_BIOTIC_STIMULUS(1675) | 3.40E-151 |
| INNATE_IMMUNE_RESPONSE(926) | 1.15E-150 |
| IMMUNE_SYSTEM_PROCESS(980) | 6.89E-149 |
| IMMUNE_RESPONSE(980) | 6.89E-149 |
| RESPONSE_TO_OTHER_ORGANISM(1411) | 2.41E-140 |
| RESPONSE_TO_STRESS(4037) | 2.61E-131 |
| RESPONSE_TO_STIMULUS(6222) | 1.89E-123 |
| DEFENSE_RESPONSE,_INCOMPATIBLE_INTERACTION(535) | 5.07E-123 |
| MULTI-ORGANISM_PROCESS(1804) | 3.98E-122 |

F

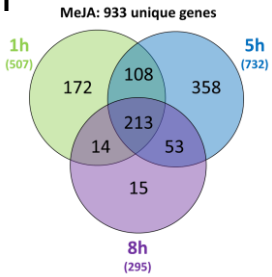


Top10 enriched GO terms

| Gene Set Name(NO. Genes) | FDR |
|---|---|
| RESPONSE_TO_JASMONIC_ACID_STIMULUS(471) | 1.46E-74 |
| RESPONSE_TO_STIMULUS(6222) | 1.46E-64 |
| RESPONSE_TO_WOUNDING(340) | 3.02E-64 |
| JASMONIC_ACID_METABOLIC_PROCESS(159) | 3.02E-64 |
| OXYLIPIN_METABOLIC_PROCESS(167) | 4.12E-64 |
| RESPONSE_TO_STRESS(4037) | 1.99E-58 |
| RESPONSE_TO_CHEMICAL_STIMULUS(3953) | 2.06E-52 |
| JASMONIC_ACID_BIOSYNTHETIC_PROCESS(135) | 9.12E-52 |
| OXYLIPIN_BIOSYNTHETIC_PROCESS(141) | 7.85E-51 |
| SMALL_MOLECULE_BIOSYNTHETIC_PROCESS(1859) | 1.01E-50 |

G

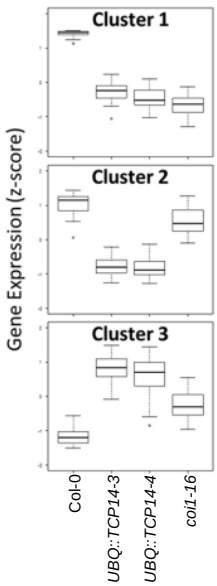


| GO Term | Description | FDR |
|---|---|---|
| GO:0009718 | anthocyanin biosynthetic process | 1.78E-05 |
| GO:0009753 | response to jasmonic acid stimulus | 1.78E-05 |
| GO:0046283 | anthocyanin metabolic process | 3.47E-05 |
| GO:0009611 | response to wounding | 8.74E-04 |
| GO:0019762 | glucosinolate catabolic process | 8.74E-04 |

No enriched terms

| | | |
|---|---|---|
| GO:0010467 | gene expression | 1.63E-05 |
| GO:0034645 | cell. macromolecule bios. process | 4.99E-05 |
| GO:0009059 | macromolecule bios. process | 3.47E-05 |
| GO:0044260 | cell. macromolecule metabolic process | 1.00E-03 |
| GO:0090304 | nucleic acid metabolic process | 1.30E-03 |

# sFigure 2

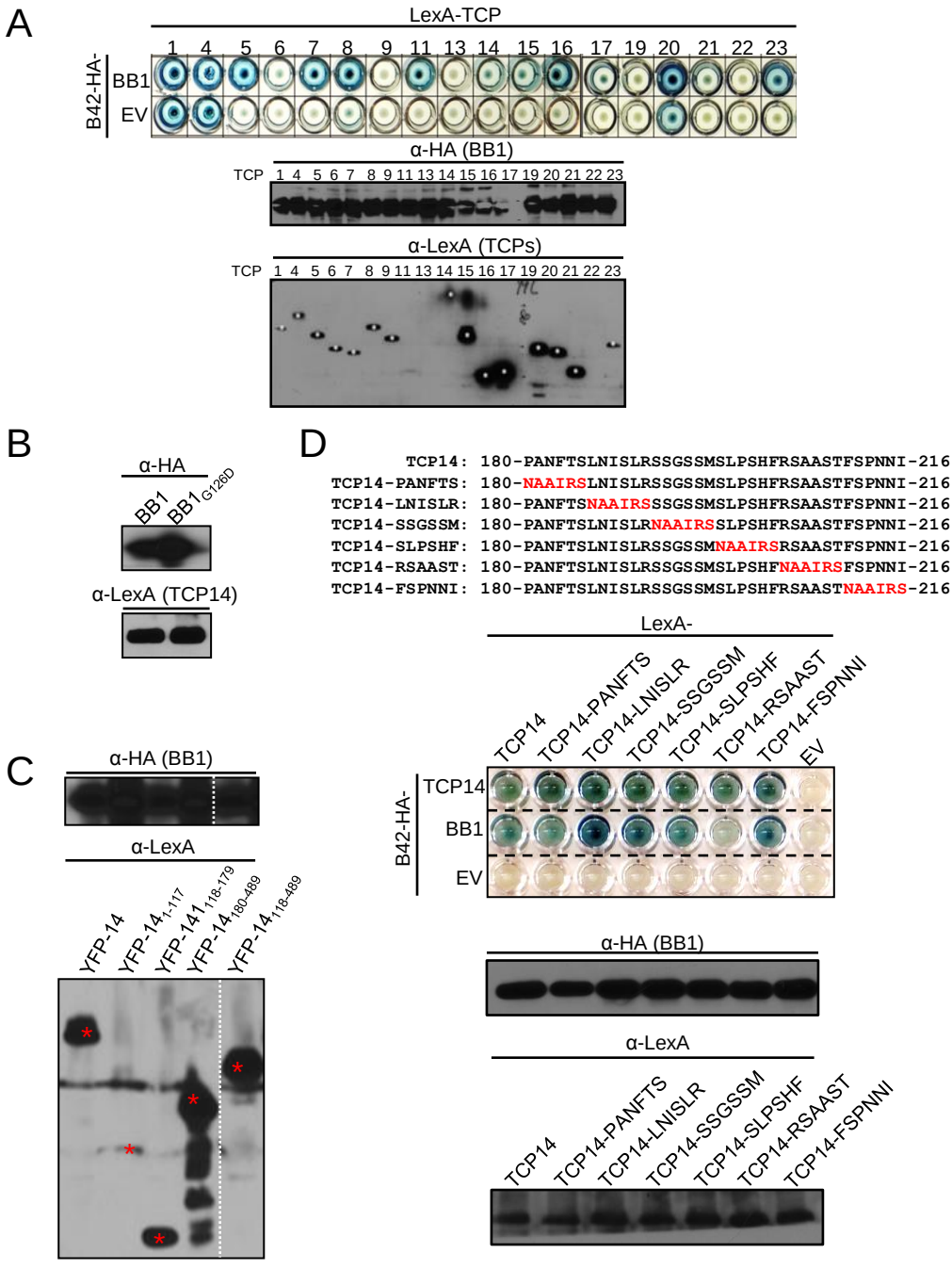
A
LexA-TCP
1 4 5 6 7 8 9 11 13 14 15 16 17 19 20 21 22 23
B42-HA-
BB1
EV
α-HA (BB1)
TCP 1 4 5 6 7 8 9 11 13 14 15 16 17 19 20 21 22 23
α-LexA (TCPs)
TCP 1 4 5 6 7 8 9 11 13 14 15 16 17 19 20 21 22 23
B
α-HA
BB1
BB1G126D
α-LexA (TCP14)
C
α-HA (BB1)
α-LexA
YFP-14
YFP-14 1-117
YFP-14 118-179
YFP-14 180-489
YFP-14 118-489
D
TCP14: 180-PANFTSLNISLRSSGSSMSLPSHFRSAASTFSPNNI-216
TCP14-PANFTS: 180-NAAIRSLNISLRSSGSSMSLPSHFRSAASTFSPNNI-216
TCP14-LNISLR: 180-PANFTSNAAIRSSSGSSMSLPSHFRSAASTFSPNNI-216
TCP14-SSGSSM: 180-PANFTSLNISLRNAAIRSSLPSHFRSAASTFSPNNI-216
TCP14-SLPSHF: 180-PANFTSLNISLRSSGSSMNAAIRSRSAASTFSPNNI-216
TCP14-RSAAST: 180-PANFTSLNISLRSSGSSMSLPSHFNAAIRSFSPNNI-216
TCP14-FSPNNI: 180-PANFTSLNISLRSSGSSMSLPSHFRSAASTNAAIRS-216
LexA-
TCP14
TCP14-PANFTS
TCP14-LNISLR
TCP14-SSGSSM
TCP14-SLPSHF
TCP14-RSAAST
TCP14-FSPNNI
EV
B42-HA-
TCP14
BB1
EV
α-HA (BB1)
α-LexA
TCP14
TCP14-PANFTS
TCP14-LNISLR
TCP14-SSGSSM
TCP14-SLPSHF
TCP14-RSAAST
TCP14-FSPNNI

# sFigure 3

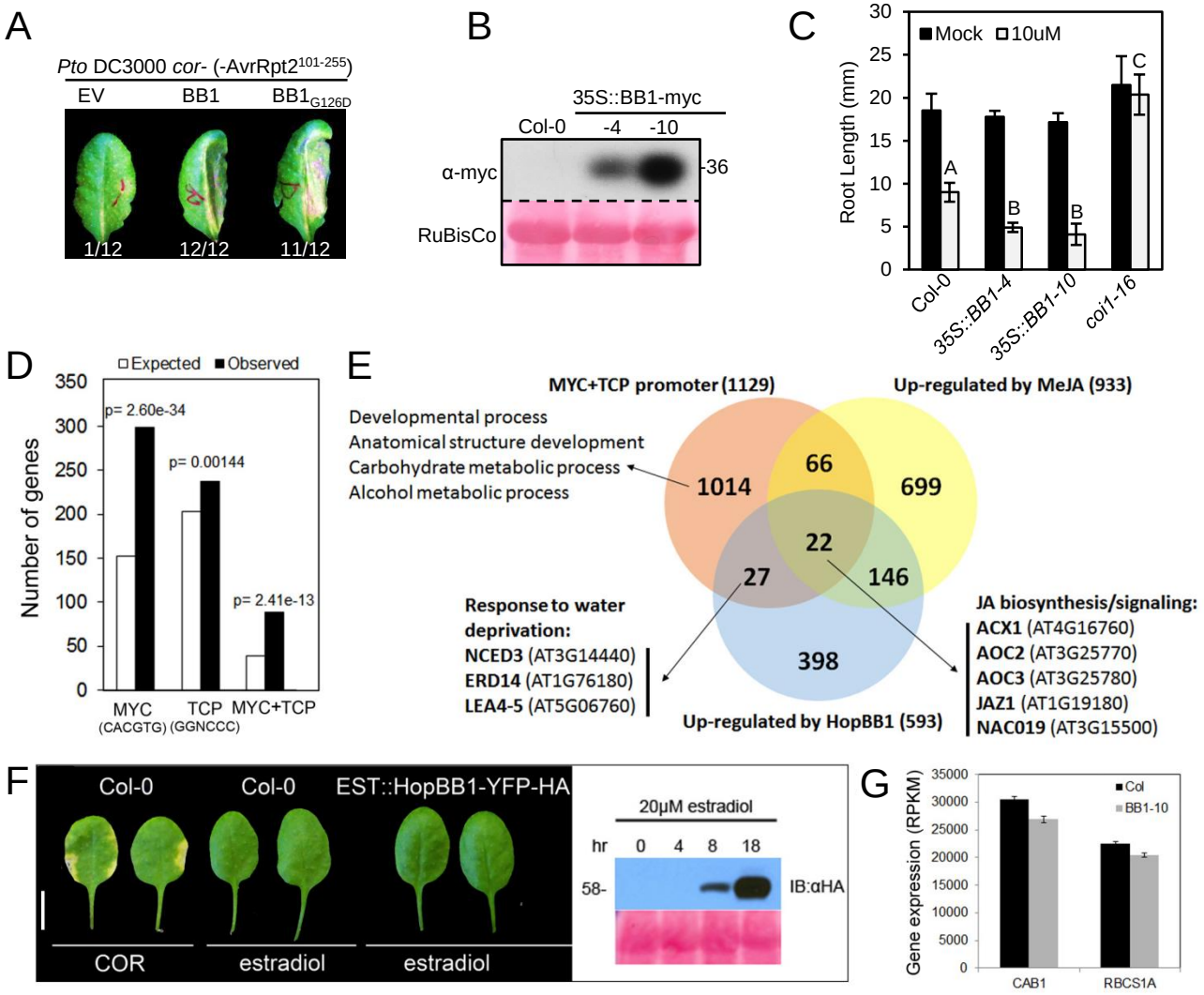
A
Pto DC3000 cor- (-AvrRpt2101-255)
EV
BB1
BB1G126D
1/12
12/12
11/12
B
35S::BB1-myc
Col-0
-4
-10
α-myc
-36
RuBisCo
C
Mock
10uM
Root Length (mm)
A
B
B
C
Col-0
35S::BB1-4
35S::BB1-10
coi1-16
D
Expected
Observed
Number of genes
p= 2.60e-34
p= 0.00144
p= 2.41e-13
MYC (CACGTG)
TCP (GGNCCC)
MYC+TCP
E
MYC+TCP promoter (1129)
Up-regulated by MeJA (933)
Developmental process
Anatomical structure development
Carbohydrate metabolic process
Alcohol metabolic process
1014
66
699
22
27
146
398
Response to water deprivation:
NCED3 (AT3G14440)
ERD14 (AT1G76180)
LEA4-5 (AT5G06760)
JA biosynthesis/signaling:
ACX1 (AT4G16760)
AOC2 (AT3G25770)
AOC3 (AT3G25780)
JAZ1 (AT1G19180)
NAC019 (AT3G15500)
Up-regulated by HopBB1 (593)
F
Col-0
Col-0
EST::HopBB1-YFP-HA
COR
estradiol
estradiol
20μM estradiol
hr
0
4
8
18
58-
IB:αHA
G
Col
BB1-10
Gene expression (RPKM)
CAB1
RBCS1A

# sFigure 4

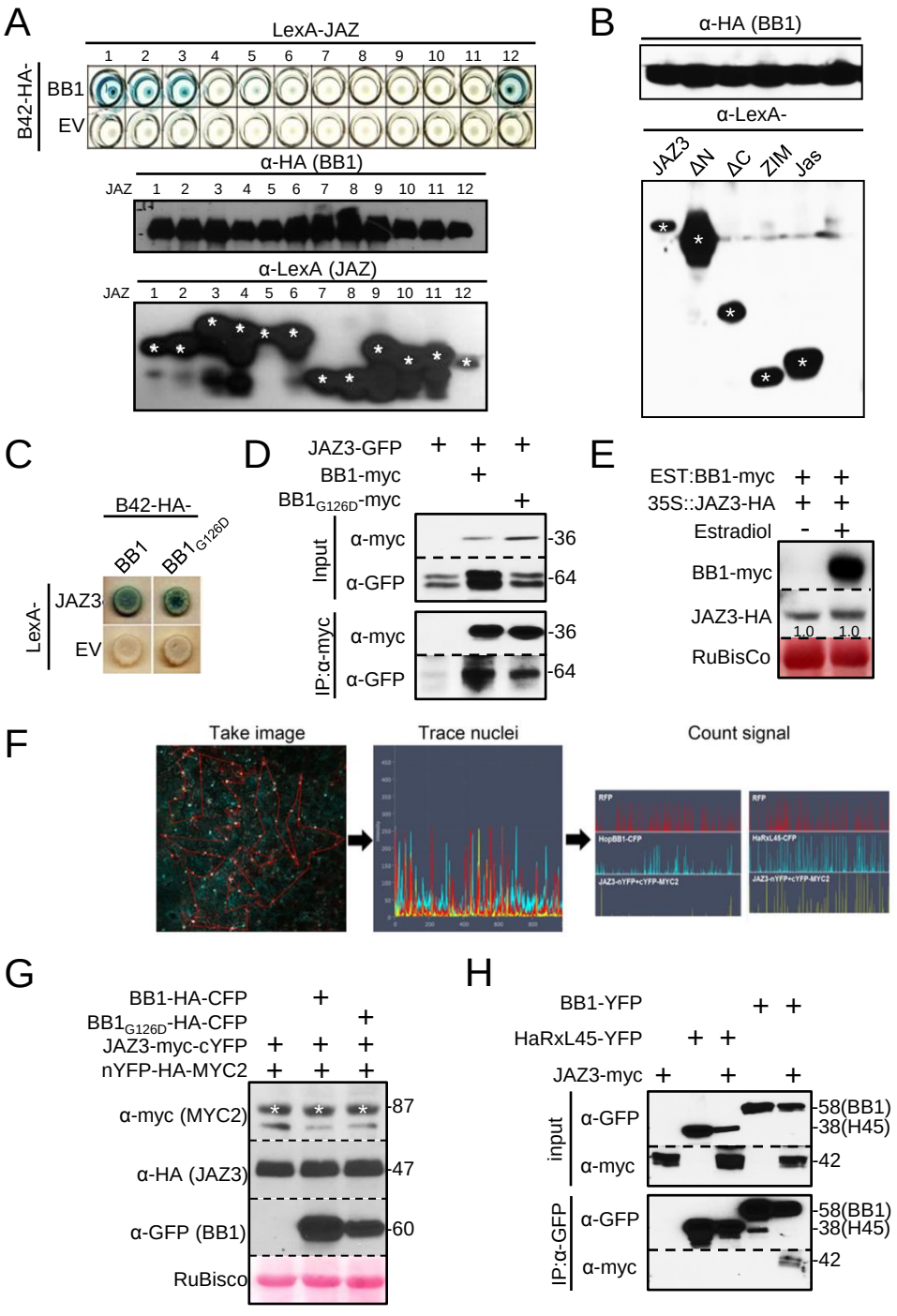
A
LexA-JAZ
1 2 3 4 5 6 7 8 9 10 11 12
B42-HA-
BB1
EV
α-HA (BB1)
JAZ 1 2 3 4 5 6 7 8 9 10 11 12
α-LexA (JAZ)
JAZ 1 2 3 4 5 6 7 8 9 10 11 12
B
α-HA (BB1)
α-LexA-
JAZ3 ΔN ΔC ZIM Jas
C
B42-HA-
BB1
BB1G126D
LexA-
JAZ3
EV
D
JAZ3-GFP + + +
BB1-myc +
BB1G126D-myc +
Input
α-myc
α-GFP
IP:α-myc
α-myc
α-GFP
-36
-64
-36
-64
E
EST:BB1-myc + +
35S::JAZ3-HA + +
Estradiol - +
BB1-myc
JAZ3-HA
1.0 1.0
RuBisCo
F
Take image
Trace nuclei
Count signal
RFP
HopBB1-CFP
JAZ3-nYFP+cYFP-MYC2
RFP
HaRxL45-CFP
JAZ3-nYFP+cYFP-MYC2
G
BB1-HA-CFP +
BB1G126D-HA-CFP +
JAZ3-myc-cYFP + + +
nYFP-HA-MYC2 + + +
α-myc (MYC2)
α-HA (JAZ3)
α-GFP (BB1)
RuBisco
-87
-47
-60
H
BB1-YFP + +
HaRxL45-YFP + +
JAZ3-myc + + +
input
α-GFP
α-myc
IP:α-GFP
α-GFP
α-myc
-58(BB1)
-38(H45)
-42
-58(BB1)
-38(H45)
-42

# sFigure 5

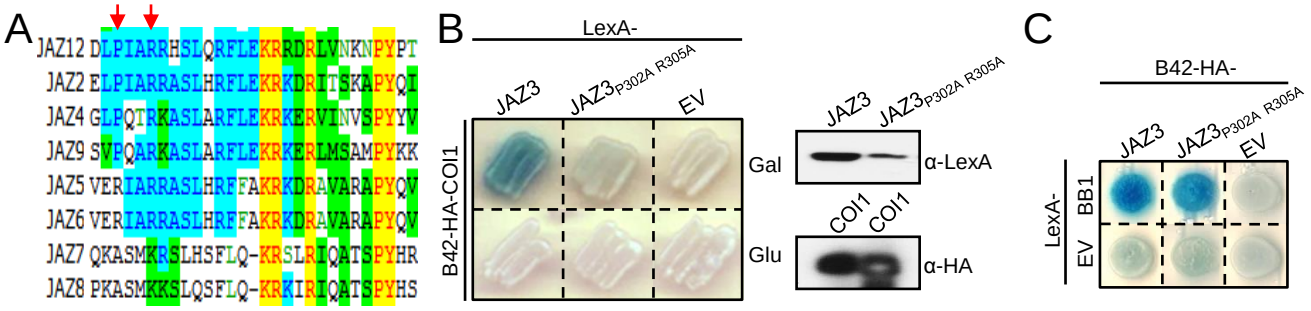
A
JAZ12 DLPIARRHSLQRFLEKRRDRLVNKNPYPT
JAZ2 ELPIARRASLHRFLEKRKDRITSKAPYQI
JAZ4 GLPQTRKASLARFLEKRKERVINVSPYYV
JAZ9 SVPQARKASLARFLEKRKERLMSAMPYKK
JAZ5 VERIARRASLHRFFAKRKDRAVARAPYQV
JAZ6 VERIARRASLHRFFAKRKDRAVARAPYQV
JAZ7 QKASMKRSLHSFLQ-KRSLRIQATSPYHR
JAZ8 PKASMKKSLQSFLQ-KRKIRIQATSPYHS
B
LexA-
JAZ3
JAZ3P302A R305A
EV
B42-HA-COI1
Gal
Glu
JAZ3
JAZ3P302A R305A
α-LexA
COI1
COI1
α-HA
C
B42-HA-
JAZ3
JAZ3P302A R305A
EV
LexA-
BB1
EV

# sFigure 6

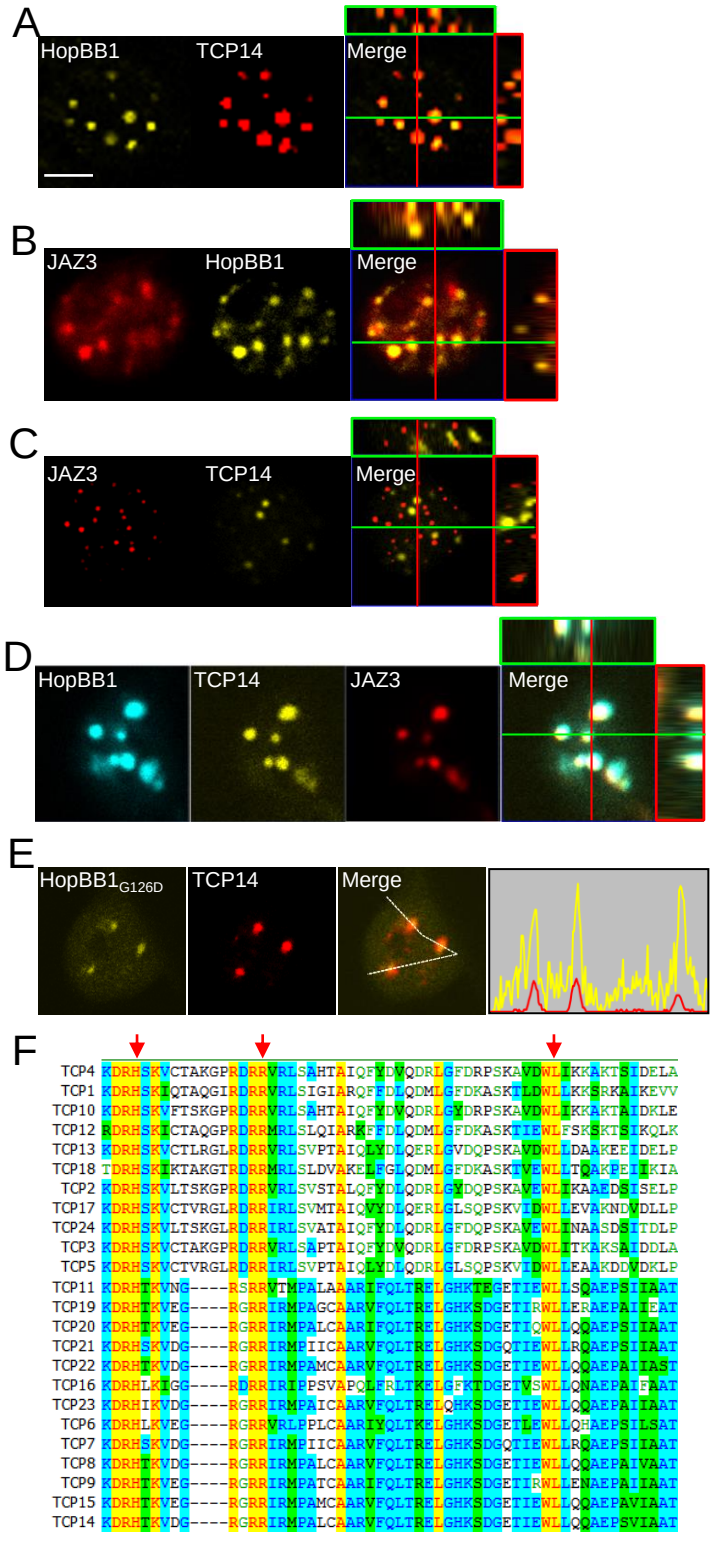
A
HopBB1
TCP14
Merge
B
JAZ3
HopBB1
Merge
C
JAZ3
TCP14
Merge
D
HopBB1
TCP14
JAZ3
Merge
E
HopBB1G126D
TCP14
Merge
F
TCP4 KDRHSKVCTAKGPRDRRVRLSAHTAIQFYDVQDRLGFDRPSKAVDWLIKKAKTSIDELA
TCP1 KDRHSKIQTAQGIRDRRVRLSIGIARQFFDLQDMLGFDKASKTLDWLLKKSRKAIKEVV
TCP10 KDRHSKVFTSKGPRDRRVRLSAHTAIQFYDVQDRLGYDRPSKAVDWLIKKAKTAIDKLE
TCP12 RDRHSKICTAQGPRDRRMRLSLQIARRFFDLQDMLGFDKASKTIEWLFSKSKTSIKQLK
TCP13 KDRHSKVCTLRGLRDRRVRLSVPTAIQLYDLQERLGVDQPSKAVDWLLDAAKEEIDELP
TCP18 TDRHSKIKTAKGTRDRRMRLSLDVAKELFGLQDMLGFDKASKTVEWLLTQAKPEIIKIA
TCP2 KDRHSKVLTSKGPRDRRVRLSVSTALQFYDLQDRLGYDQPSKAVEWLIKAAEDSISELP
TCP17 KDRHSKVCTVRGLRDRRIRLSVMTAIQVYDLQERLGLSQPSKVIDWLLEVAKNDVDLLP
TCP24 KDRHSKVLTSKGLRDRRIRLSVATAIQFYDLQDRLGFDQPSKAVEWLINAASDSITDLP
TCP3 KDRHSKVCTAKGPRDRRVRLSAPTAIQFYDVQDRLGFDRPSKAVDWLITKAKSAIDDLA
TCP5 KDRHSKVCTVRGLRDRRIRLSVPTAIQLYDLQDRLGLSQPSKVIDWLLEAAKDDVDKLP
TCP11 KDRHTKVNG----RSRRVTMPALAAARIFQLTRELGHKTEGETIEWLLSQAEPSIIAAT
TCP19 KDRHTKVEG----RGRRIRMPAGCAARVFQLTRELGHKSDGETIRWLLERAEPAIIEAT
TCP20 KDRHTKVEG----RGRRIRMPALCAARIFQLTRELGHKSDGETIQWLLQQAEPSIIAAT
TCP21 KDRHSKVDG----RGRRIRMPIICAARVFQLTRELGHKSDGQTIEWLLRQAEPSIIAAT
TCP22 KDRHTKVDG----RGRRIRMPAMCAARVFQLTRELGHKSDGETIEWLLQQAEPAIIAST
TCP16 KDRHLKIGG----RDRRIRIPPSVAPQLFRLTKELGFKTDGETVSWLLQNAEPAIFAAT
TCP23 KDRHIKVDG----RGRRIRMPAICAARVFQLTRELQHKSDGETIEWLLQQAEPAIIAAT
TCP6 KDRHLKVEG----RGRRVRLPPLCAARIYQLTKELGHKSDGETLEWLLQHAEPSILSAT
TCP7 KDRHSKVDG----RGRRIRMPIICAARVFQLTRELGHKSDGQTIEWLLRQAEPSIIAAT
TCP8 KDRHTKVDG----RGRRIRMPALCAARVFQLTRELGHKSDGETIEWLLQQAEPAIVAAT
TCP9 KDRHTKVEG----RGRRIRMPATCAARIFQLTRELGHKSDGETIRWLLENAEPAIIAAT
TCP15 KDRHTKVEG----RGRRIRMPAMCAARVFQLTRELGHKSDGETIEWLLQQAEPAVIAAT
TCP14 KDRHTKVDG----RGRRIRMPALCAARVFQLTRELGHKSDGETIEWLLQQAEPSVIAAT
G
LexA-
TCP14
TCP14H121Q R130K L161N
EV
B42-HA-
TCP14
BB1
EV
H
BB1-YFP + + +
TCP14-HA + + +
TCP14H121Q R130K L161N-HA + +
input
α-GFP
α-HA
IP:α-GFP
α-GFP
α-HA
60
56
60
56
I
TCP14H121Q R130K L161N-GFP + +
TCP14H121Q R130K L161N-HA + +
input
α-GFP
α-HA
IP:α-GFP
α-GFP
α-HA
80
56
80
56

**Figure S1 (Related to Figure 1)**

(A) Accumulation of YFP-TCP14 protein (left) and transcripts (right) in transgenic plants. Error bars represent ±SD.

(B)–(F) Defining JA and SA responsive genes in Col-0. (B) Overview of the experimental conditions used to define genes responsive to MeJA and BTH by RNA-seq. (C) Principal Component Analysis (PCA) showing the overall relationship of the RNA-seq libraries used to define MeJA and BTH/SA markers. Colors represent different time-points and symbols represent treatments. Biological replicates are labeled r1 and r2. (D) Number of genes up- and down-regulated by each treatment defined using the edgeR package (FDR ≤ 0.01; 1.5 fold-change difference). While 261 genes were up-regulated by both hormones, 672 and 2096 genes were up-regulated specifically by MeJA and BTH, respectively, which define our set of marker genes. Table S1 shows the complete RNA-seq results for all Arabidopsis genes. (E) Overview of genes up-regulated by BTH at each time-point. The table shows Gene Ontology terms (biological processes) enriched in this set of genes. (F) Overview of the genes up-regulated by MeJA at each time-point. The table shows Gene Ontology terms (biological processes) enriched in this set of genes.

(G) Gene Ontology terms (biological processes) enriched in the set of genes identified as differentially expressed in the *UBQ::YFP-TCP14-3* line. The three clusters correspond to the hierarchical clustering analysis presented in Figure 1D.

**Figure S2 (Related to Figure 2)**

(A) Protein interaction between HopBB1 and 18 of 24 Arabidopsis TCP family members in yeast.

(B) Protein accumulation in Figure 2B.

(C) Protein accumulation in Figure 2D.

(D) NAAIRS-scanning mutagenesis in the $TCP14_{180\text{-}216}$ region. $TCP14_{RSAAST/NAAIRS}$ cannot interact with HopBB1.

**Figure S3 (Related to Figure 3)**

(A) HopBB1 and $HopBB1_{G126D}$ were delivered into plant cells when expressed in *Pto* DC3000 *cor*-. HopBB1 or $HopBB1_{G126D}$ were cloned upstream of $AvrRpt2^{101\text{-}255}$. The chimeric proteins were expressed under the control of NPTII promoter (Vinatzer et al., 2005).

(B) Protein accumulation in transgenic plants expressing HopBB1-myc.

(C) Plants expressing HopBB1 are hypersensitive to JA-mediated inhibition of root elongation. One-week-old seedlings grown on vertical plates were transferred to mock plates or plates with 10μM MeJA. Root length was measured one week after transfer. Error bars indicate ±SD. Statistics were performed using one-way ANOVA test with Tukey-Kramer HSD with 95% confidence. Similar results were obtained from two independent experiments.

(D) Co-occurrence of consensus MYC (CACGTG) and TCP (GGNCCC) binding sites is enriched in the promoters of MeJA-regulated genes from Figure S1F,

Table S1 (88/933, p=2.41e-13; hypergeometric test). We searched for these motifs in the 1kb upstream region relative to the start codon of 27206 nuclear protein-coding genes (TAIR10). The observed number of promoters containing each or both motifs was contrasted to the expected number in each category, given the motif's frequency in the entire genome and tested for over-representation using the hypergeometric test.

(E) The overlap between genes up-regulated by MeJA and HopBB1, and with the co-occurrence of TCP14 and MYC binding sites in their promoters. We verified that 22 (25%) of the 88 JA-responsive genes containing both MYC and TCP binding sites in their promoters are also up-regulated by HopBB1, which is more than expected by random sampling (2.18%; p=1.49e-16; hypergeometric test). Importantly, this list includes genes required for JA biosynthesis and signaling.

(F) Induced expression of HopBB1 does not trigger chlorosis (left). Four-week old plants were either treated with 50µM of coronatine or 20µM of estradiol for five days. The fifth leaves from three representative plants were photographed. Bar=5mm. The protein accumulation of conditionally expressed HopBB1 is shown in the right panel.

(G) The expression of representative photosynthesis genes is not altered in HopBB1-myc expressing plants.

**Figure S4 (Related to Figure 5)**

(A) Protein interaction between HopBB1 and 12 Arabidopsis JAZ family members in yeast. HopBB1 interacts with a subset of JAZ proteins.

(B) Protein accumulation for Figure 5C.

(C) $HopBB1_{G126D}$ retains interaction with JAZ3 in yeast.

(D) $HopBB1_{G126D}$ retains interaction with JAZ3 in *N. benthamiana*.

(E) HopBB1 does not promote JAZ3 degradation in Arabidopsis. Conditional expression of HopBB1-myc in transgenic plants expressing 35S::JAZ3-HA does not alter the accumulation of JAZ3.

(F) Quantification of the HopBB1-mediated disruption of MYC2-JAZ3 association. Proteins were transiently co-expressed in *N. benthamiana*. HaRxL45-CFP, HopBB1-CFP or $HopBB1_{G126D}$-CFP was induced 6 hrs after Agrobacteria infiltration. Microscopy was conducted 18 hrs after induction. Eight to ten confocal images with 1 $mm^2$ field of view were taken from four randomly sampled leaf discs on each leaf. Images were taken from YFP, CFP and RFP channels. Nuclei were traced only in the RFP channel. Following that, the nucleus signal peaks in each individual channel were counted, and the degree of overlap was compared. Four independent experiments were pooled for the summary presented in Figure 5F.

(G) HopBB1 does not alter MYC2 level in *N. benthamiana*. Proteins were transiently co-expressed in *N. benthamiana.*

(H) JAZ3 does not associate with HaRxL45 *in planta*. Proteins were transiently co-expressed in *N. benthamiana* from a constitutive 35S promoter.

**Figure S5 (Related to Figure 6)**

(A) Alignment of the conserved Jas motifs from 12 Arabidopsis JAZ proteins. The P302 and R305 are highlighted with a red arrow.

(B) $JAZ3_{P302A\ R305A}$ cannot interact with COI1 in the presence of coronatine. 50μM of coronatine was added to yeast medium. Protein accumulation is shown in the right panel.

(C) $JAZ3_{P302A\ R305A}$ interacts with HopBB1 in yeast.

**Figure S6 (related to Figure 7)**

(A) Orthogonal slices of TCP14-RFP and HopBB1-YFP co-localization in sub-nuclear foci. Bar=5 μM. For all orthogonal slices in (A)-(D), the “Merge” panel is the xy plane, right panel (red) is the yz plane, and top panel (green) is the xz plane. The crosshairs indicate the location of the yz and xz planes.

(B) Orthogonal slices view of JAZ3-RFP and HopBB1-YFP co-localization in sub-nuclear foci.

(C) Orthogonal slices view of the distinct sub-nuclear localization of TCP14-YFP and JAZ3-RFP in a nucleus.

(D) Orthogonal slices view of the co-localization of TCP14-YFP, HopBB1-CFP and JAZ3-RFP in sub-nuclear foci.

(E) $HopBB1_{G126D}$ co-localizes with TCP14 when transiently co-expressed in *N.benthamiana*.

(F) Alignment of the TCP domain from 24 Arabidopsis TCP family members. The mutated H121, R130 and L161 were highlighted with a red arrow. These

residues are conserved in TCP14. Mutation in each individual residue significantly reduced the ability of TCP4 protein to bind DNA (Kosugi and Ohashi, 2002).

(G) $TCP14_{H121Q\ R130K\ L161N}$ retains the ability to interact with HopBB1 and TCP14 in yeast.

(H) $TCP14_{H121Q\ R130K\ L161N}$ retains the ability to interact with HopBB1 in *N. benthamiana*.

(I) $TCP14_{H121Q\ R130K\ L161N}$ homo-dimerizes.

A-E, H-I: Proteins were transiently expressed from the 35S promoter in *N. benthamiana*.

**Table S1 (related to Figure 1):** Transcriptional response to MeJA or BTH in Col-0.

**Table S2 (related to Figure 1):** Transcriptional changes induced by *TCP14* mutation or overexpression.

**Table S3 (related to Figure 3):** Transcriptional changes induced by bacteria delivered HopBB1 or heterologous HopBB1 expression in Arabidopsis.

**Table S4 (related to Figure 3):** Comparison between genes expression altered by HopBB1 and TCP14 expression.

**Table S5 (related to Figure 3):** Distribution of JA-activating virulence factors in 287 *Psy* genomes.

**Table S6 (related to experimental procedures):** Primers, seed stocks, constructs, sequences and core genes for phylogenetic analysis.

## Extended Experimental Procedures

*Plants*

Arabidopsis Col-0, *tcp14-6* (SAIL_1145_H03, backcrossed to Col-0 four times) (Mukhtar et al., 2011), *tcp14-7* (cs108688, backcrossed to Col-0 twice) (Wessling et al., 2014), *coi1-16* (Ellis and Turner, 2002; He et al., 2012), and all transgenics were sown and grown as described (Boyes et al., 1998). Primers for genotyping and constructs for generating transgenic Arabidopsis were listed in Table S6.

*Yeast two hybridization*

HopBB1, JAZ3, TCP14, COI1 and mutant derivatives were cloned into gateway-compatible pJG4-5 (-Trp) or pEG202 (-His) vectors. pJG4-5 and pEG202 constructs were transformed into competent yeast strains EGY48 and RFY206, respectively following manufacturer's protocol (Frozen-EZ Yeast Transformation II ™, Zymo Research) and selected on plates with dropout media. Each strain also carries the GAL4 reporter on psH18-34 (-Ura). Positive colonies were verified by yeast colony PCR. After mating the strain EGY48 and RFY206, diploid yeasts were plated on selective medium (-H-W-U) supplied with 100μM X-Gal for developing blue color from 2-6 days. To measure protein accumulation, yeast colonies were suspended in 50 μl 0.2N NaOH for 10 minutes. Cells were then collected by centrifugation and re-suspended in 1 x loading buffer. Protein levels were examined by western blotting.

*RNA sequencing*

In order to define a comprehensive set of marker genes for the JA and SA responses, we used RNA-seq to assess the transcriptome of the Arabidopsis Col-0 ecotype over a time-course hormone treatment (Figure S1B). Two-week-old seedlings were sprayed with 50 µM MeJA (Sigma), 300 µM BTH (Actigard 50WG) or a mock solution (0.02% Silwet, 0.1% ethanol). Samples were harvested 1h, 5h and 8h after spraying. This experiment was repeated twice. The experiments shown in Figures 1D, 1E and 1F were performed using steady-state seedlings grown under the same conditions as the ones used in the hormone treatment experiment. Lines Col-0 (4 replicates), UBQ10::YFP-TCP14-3 (4 replicates), UBQ10::YFP-TCP14-4 (1 replicate), and *coi1-16* (2 replicates) were used in the experiment presented in Figures 1D and E; whereas Col-0 (3 replicates), *tcp14-6* (3 replicates) and *tcp14-7* (3 replicates) were used in the experiment shown in Figure 1F. Bacteria-infected plants were used in the experiments shown in Figures 1G, 1H and 1I. For this, the strain *Pto* DC3000 *cor-* (at $OD_{600}$=0.2 with 10mM $MgCl_2$ and 0.04% Silwet L-77) was sprayed onto Col-0 (3 replicates), *tcp14-6* (3 replicates), UBQ10::YFP-TCP14-4 (3 replicates) and *coi1-16* (3 replicates). Samples were harvested for RNA preparation 24 hours post infection.

We also evaluated the effect of bacteria-delivered HopBB1 on the transcriptome of wild-type plants (shown in Figures 3B, 3C and 3D). For this, two-week-old Col-0 seedlings were sprayed with a mock solution (10 mM $MgCl_2$) or bacteria [*Pto* DC3000 (EV), *Pto* DC3000 *cor-* (EV); *Pto* DC3000 *cor-* (HopBB1); *Pto* DC3000 *cor-* ($HopBB1_{G126D}$)] at $OD_{600}$=0.2 with 10mM $MgCl_2$ and 0.04% Silwet L-77.

Samples were harvested 24 hours after infection. This experiment included three biological replicates. The transcriptome of the transgenic line HopBB1-myc-10 (3 replicates) was also compared to the one of Col-0 seedlings at steady-state conditions (shown in Figure 3G). In all experiments, each biological replicate corresponds to approximately 30 seedlings grown on the same pot.

For RNA isolation, plant tissue was ground to a fine powder using the Qiashredder tissue homogenizer (Qiagen) and total RNA was extracted using the RNeasy Plant Mini kit (Qiagen). Illumina-based RNA-seq libraries were prepared from 1000ng total RNA. Library quality control and quantification were performed using a 2100 Bioanalyzer instrument (Agilent) and the Quant-iT PicoGreen dsDNA Reagent (Invitrogen), respectively. The Illumina HiSeq2500 sequencer was used to generate single-end reads. Raw sequencing data are available at the NCBI Gene Expression Omnibus GEO:GSE90606.

RNA-seq reads were mapped against the TAIR10 reference genome using Tophat (Trapnell et al., 2009). Alignment parameters were set to allow only one mismatch and to discard reads mapping to multiple positions in the reference. HTSeq (Anders et al., 2015) was then used to count reads mapping to each one of the 27,206 nuclear protein-coding genes. Differential gene expression analyses were performed with the edgeR package (Robinson et al., 2010) using the False Discovery Rate (FDR) method for correction of multiple comparisons (Benjamini and Hochberg, 1995). Genes with FDR below 0.01 and a fold-change variation greater than 1.5X were considered differentially expressed between conditions. Gene Ontology enrichment analyses were performed with the

PlantGSEA toolkit (Yi et al., 2013) and with the Cytoscape plugin ClueGO (Bindea et al., 2009) .

We identified a total of 933 and 2357 genes that were significantly up-regulated (FDR≤0.01; 1.5 fold-change difference relative to the mock control) in at least one of the three time-points analyzed after treatment with MeJA or BTH, respectively (Figure S1D; Table S1). As expected, these sets of genes were strongly enriched for biological processes related to JA and SA responses (Figures S1E and S1F). After filtering out the 261 genes upregulated by both hormones, we defined a set of 672 and 2096 markers of the JA and SA responses, respectively.

*Confocal microscopy*

Microscopy was conducted 16-24 hours after infiltration using a LSM 7 DUO (Carl Zeiss). Leaf disc samples were imaged with a 40x water objective. Between 5 and 15 nuclei were observed in each repetition. The confocal images were edited with Zen 2009 (Zeiss) and Adobe Photoshop CS2. Zen 2009 (Zeiss) and Excel (Microsoft) were used to create histograms. For the HopBB1-TCP14-JAZ3 co-localization assay, JAZ3-RFP and TCP14-YFP were driven under 35S promoter, HopBB1-CFP or $HopBB1_{G126D}$-CFP was driven by estradiol-inducible promoter. Estradiol was applied 6 hours after the co-infiltration of Agrobacteria. The primers and constructs used for confocal analysis are listed in Table S6. GV3101 carrying 35S promoter-driven p19 protein was co-infiltrated at

89 $OD_{600}$=0.05 in each experiment to prevent the onset of post-transcriptional gene
90 silencing and improve the efficiency of transient expression (Lindbo, 2007).
91
92 For transient protein expression in *N. benthamiana*, Agrobacteria at annotated
93 concentration were suspended in 10mM $MgCl_2$, 10mM MES and 100μM
94 acetosyringone, and hand infiltrated into *N. benthamiana* leaves. For the
95 HopBB1-mediated disruption of the JAZ3-MYC2 interaction, rBiFC (JAZ3+MYC2)
96 and EST::HopBB1-CFP-HA, EST::HopBB1$_{G126D}$-CFP-HA or EST::HaRxL45-CFP-
97 HA were co-inoculated at $OD_{600}$=0.1 and $OD_{600}$=0.2, respectively (Grefen and
98 Blatt, 2012). Six hours after inoculation, 20μM estradiol was infiltrated. Samples
99 were collected 20-24 hours after inoculation. 4-6 images of 50-80 cells/per field
100 were taken in each repetition.
101
102 *Disease resistance assay*

103 *Pto* DC3000 *and Pto* DC3000 *cor-* were described in (He et al., 2012). *Pto*
104 DC3000 *cor-* (EV), *Pto* DC3000 *cor-* (HopBB1) and *Pto* DC3000 *cor-*
105 (HopBB1$_{G126D}$) were generated by transforming *Pto* DC3000 *cor-* with either
106 pJC531 (empty vector), pJC531 (HopBB1) or pJC531 (HopBB1$_{G126D}$). HopBB1 or
107 HopBB1$_{G126D}$ were expressed from the native promoter. Bacterial growth assays
108 in *Arabidopsis* were performed by spray or dipping inoculation as described.
109 Bacterial cultures were resuspended in 10 mM $MgCl_2$ with 0.04% Silwet L-77.
110 Plants were sprayed or dipped with a bacterial suspension at $OD_{600}$=0.2. Results
111 displayed in Figures 1C, 3A and 3F were performed independently a minimum of

3 times with similar results. Hpa infection was performed as described in (Mukhtar et al., 2011).

Bacterial colony formation units (CFU) were measured after three days. Dashed line indicates the CFU at day 0. Statistics in Figures 1C, 3A and 3F were performed using one-way ANOVA test with Tukey-Kramer HSD with 95% confidence.

*Effector Delivery Assay*

The coding regions of HopBB1 or $HopBB1_{G126D}$ were cloned into pBAV178 (proNPTII:: Gateway cassette-$AvrRpt2^{101-255}$) (Vinatzer et al., 2005). pBAV178 (HopBB1) and pBAV178 ($HopBB1_{G126D}$) were transformed into *Pto* DC3000 *cor-.* Bacteria were infiltrated into leaves of four-week-old Col-0 plants at $OD_{600}$=0.01 with 10mM $MgCl_2$, and cell death was scored after 16-20 hours.

*Phylogenetic Analysis*

The phylogenetic history of *Pseudomonas* was inferred by multi-locus alignment using MUSCLE (Edgar, 2004) to align amino acid sequences of 31 single copy core genes from the 2681 *Pseudomonas* genomes available for download on the PATRIC database (Wattam et al., 2014) . Using the resulting tree, *P. syringae* genomes were identified by selecting the smallest monophyletic group containing all genomes annotated as *P. syringae*. This analysis resulted in a dataset 287 *P. syringae* genomes (Table S5). Pan genome analysis was performed on this subset using Roary (Page et al., 2015) with default parameters. The nucleotide

sequences of the resulting 84 core genes (Table S6) were used to construct a new phylogenetic tree. Trees were constructed using a Maximum Likelihood method (Jones et al., 1992) implemented in MEGA7 (Tamura et al., 2013) with 100 bootstrap iterations. The HopBB1 (from *Pseudomonas syringae pv. mori str.* 301020), HopX1 (from *Pseudomonas syringae pv. tabaci str. ATCC* 11528), HopZ1a (from *Pseudomonas syringae pv. syringae* strain A2) and the coronatine biosynthesis pathway genes (from *Pseudomonas syringae pv. tomato str.* DC3000) were used as blast queries to search for homologous proteins in these 287 *P. syringae* genomes. A hit with over 80% protein sequence identity was considered positive. For HopZ1a, the difference between HopZ1a and HopZ1b annotated in (Ma et al., 2006) was used as guideline. Each homologue was manually checked for the integrity of reading frame. The tree was visualized using iTOL (http://itol.embl.de/) (Letunic and Bork, 2007) . A newick file is available for download and interactive viewing at http://itol.embl.de/shared/HopBB1.

## References

Anders, S., Pyl, P.T., and Huber, W. (2015). HTSeq--a Python framework to work with high-throughput sequencing data. Bioinformatics *31*, 166-169.

Benjamini, Y., and Hochberg, Y. (1995). Controlling the false discovery rate: a practical and powerful approach to multiple testing. Journal of the Royal Statistical Society. Series B (Methodological), 289-300.

Bindea, G., Mlecnik, B., Hackl, H., Charoentong, P., Tosolini, M., Kirilovsky, A., Fridman, W.H., Pages, F., Trajanoski, Z., and Galon, J. (2009). ClueGO: a Cytoscape plug-in to decipher functionally grouped gene ontology and pathway annotation networks. Bioinformatics *25*, 1091-1093.

Boyes, D.C., Nam, J., and Dangl, J.L. (1998). The Arabidopsis thaliana RPM1 disease resistance gene product is a peripheral plasma membrane protein that is degraded coincident with the hypersensitive response. Proc. Natl. Acad. Sci. USA *95*, 15849-15854.

Edgar, R.C. (2004). MUSCLE: multiple sequence alignment with high accuracy and high throughput. Nucleic Acids Res. *32*, 1792-1797.

Ellis, C., and Turner, J.G. (2002). A conditionally fertile coi1 allele indicates cross-talk between plant hormone signalling pathways in Arabidopsis thaliana seeds and young seedlings. Planta *215*, 549-556.

Grefen, C., and Blatt, M.R. (2012). A 2in1 cloning system enables ratiometric bimolecular fluorescence complementation (rBiFC). Biotechniques *53*, 311-314.

He, Y., Chung, E.H., Hubert, D.A., Tornero, P., and Dangl, J.L. (2012). Specific missense alleles of the arabidopsis jasmonic acid co-receptor COI1 regulate innate immune receptor accumulation and function. PLoS Genet. *8*, e1003018.

Jones, D.T., Taylor, W.R., and Thornton, J.M. (1992). The rapid generation of mutation data matrices from protein sequences. Comput Appl. Biosci. *8*, 275-282.

Letunic, I., and Bork, P. (2007). Interactive Tree Of Life (iTOL): an online tool for phylogenetic tree display and annotation. Bioinformatics *23*, 127-128.

Lindbo, J.A. (2007). High-efficiency protein expression in plants from agroinfection-compatible Tobacco mosaic virus expression vectors. BMC Biotechnol. *7*, 52.

184 Ma, W., Dong, F.F., Stavrinides, J., and Guttman, D.S. (2006). Type III effector
185 diversification via both pathoadaptation and horizontal transfer in response to a
186 coevolutionary arms race. PLoS Genet. *2*, e209.

187 Mukhtar, M.S., Carvunis, A.R., Dreze, M., Epple, P., Steinbrenner, J., Moore, J.,
188 Tasan, M., Galli, M., Hao, T., Nishimura, M.T.*, et al.* (2011). Independently
189 evolved virulence effectors converge onto hubs in a plant immune system
190 network. Science *333*, 596-601.

191 Page, A.J., Cummins, C.A., Hunt, M., Wong, V.K., Reuter, S., Holden, M.T.,
192 Fookes, M., Falush, D., Keane, J.A., and Parkhill, J. (2015). Roary: rapid large-
193 scale prokaryote pan genome analysis. Bioinformatics *31*, 3691-3693.

194 Robinson, M.D., McCarthy, D.J., and Smyth, G.K. (2010). edgeR: a Bioconductor
195 package for differential expression analysis of digital gene expression data.
196 Bioinformatics *26*, 139-140.

197 Tamura, K., Stecher, G., Peterson, D., Filipski, A., and Kumar, S. (2013). MEGA6:
198 Molecular Evolutionary Genetics Analysis version 6.0. Mol. Biol. Evol. *30*, 2725-
199 2729.

200 Trapnell, C., Pachter, L., and Salzberg, S.L. (2009). TopHat: discovering splice
201 junctions with RNA-Seq. Bioinformatics *25*, 1105-1111.

202 Vinatzer, B.A., Jelenska, J., and Greenberg, J.T. (2005). Bioinformatics correctly
203 identifies many type III secretion substrates in the plant pathogen Pseudomonas
204 syringae and the biocontrol isolate P. fluorescens SBW25. Mol. Plant Microbe
205 Interact. *18*, 877-888.

206 Wattam, A.R., Abraham, D., Dalay, O., Disz, T.L., Driscoll, T., Gabbard, J.L.,
207 Gillespie, J.J., Gough, R., Hix, D., Kenyon, R.*, et al.* (2014). PATRIC, the
208 bacterial bioinformatics database and analysis resource. Nucleic Acids Res. *42*,
209 D581-591.

210 Wessling, R., Epple, P., Altmann, S., He, Y., Yang, L., Henz, S.R., McDonald, N.,
211 Wiley, K., Bader, K.C., Glasser, C.*, et al.* (2014). Convergent targeting of a
212 common host protein-network by pathogen effectors from three kingdoms of life.
213 Cell Host Microbe *16*, 364-375.

214 Yi, X., Du, Z., and Su, Z. (2013). PlantGSEA: a gene set enrichment analysis
215 toolkit for plant community. Nucleic Acids Res. *41*, W98-103.

216